iScience

CellPress
OPEN ACCESS

Article

Nutrient infusion in the dorsal vagal complex controls hepatic lipid and glucose metabolism in rats

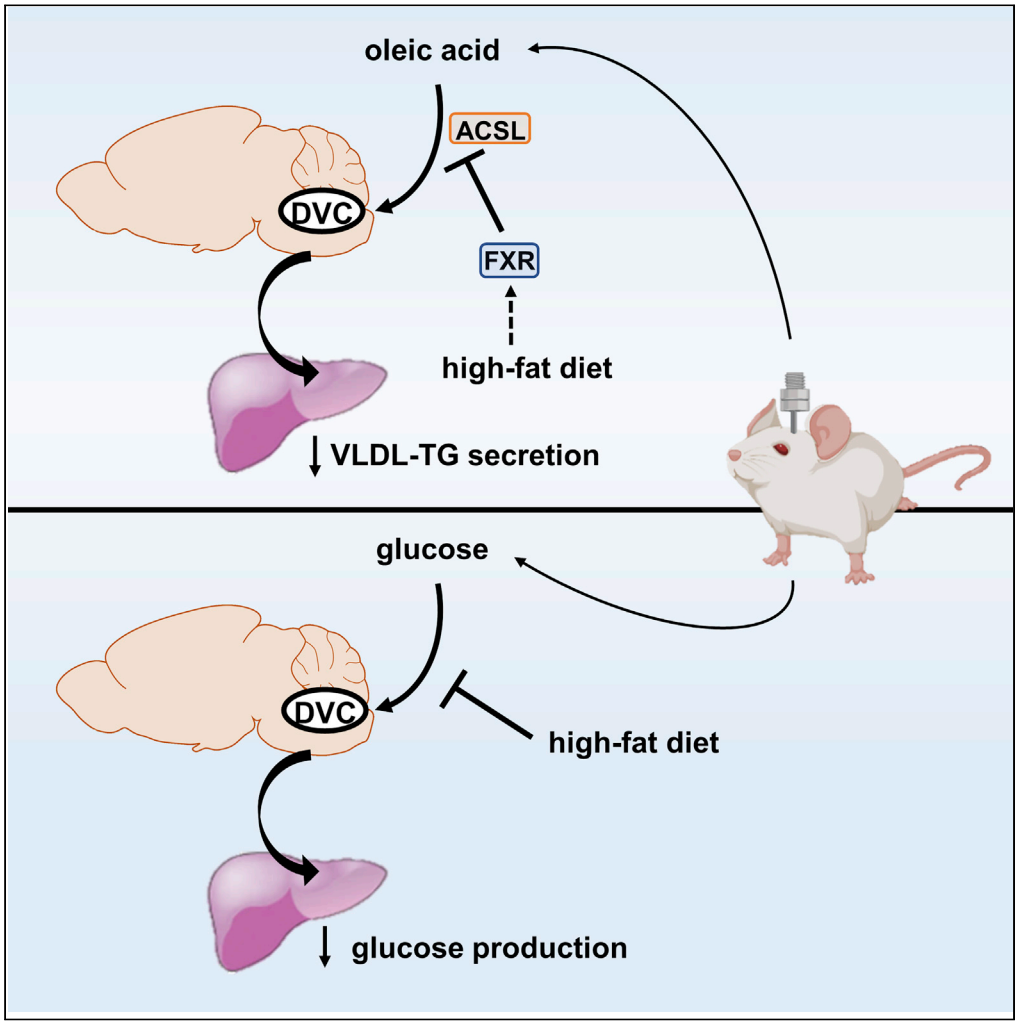

Rosa J.W. Li, Battsetseg Batchuluun, Song-Yang Zhang, ..., Yu-Mi Lim, Jessica T.Y. Yue, Tony K.T. Lam

tony.lam@uhnresearch.ca

Highlights

DVC oleic acid infusion lowers hepatic secretion of VLDL-TG in chow but not HF rats

Inhibition of ACSL in the DVC negates lipid sensing

DVC glucose infusion lowers hepatic glucose production in chow but not HF rats

Inhibition of FXR in the DVC enhances oleic acid but not glucose sensing in HF rats

Li et al., iScience *24*, 102366
April 23, 2021
https://doi.org/10.1016/j.isci.2021.102366

iScience

CellPress
OPEN ACCESS

Article

Nutrient infusion in the dorsal vagal complex controls hepatic lipid and glucose metabolism in rats

Rosa J.W. Li,[1,2] Battsetseg Batchuluun,[2] Song-Yang Zhang,[2] Mona A. Abraham,[1,2] Beini Wang,[1,2] Yu-Mi Lim,[2,3] Jessica T.Y. Yue,[4] and Tony K.T. Lam[1,2,5,6,7,*]

SUMMARY

Hypothalamic regulation of lipid and glucose homeostasis is emerging, but whether the dorsal vagal complex (DVC) senses nutrients and regulates hepatic nutrient metabolism remains unclear. Here, we found in rats DVC oleic acid infusion suppressed hepatic secretion of triglyceride-rich very-low-density lipoprotein (VLDL-TG), which was disrupted by inhibiting DVC long-chain fatty acyl-CoA synthetase that in parallel disturbed lipid homeostasis during intravenous lipid infusion. DVC glucose infusion elevated local glucose levels similarly as intravenous glucose infusion and suppressed hepatic glucose production. This was independent of lactate metabolism as inhibiting lactate dehydrogenase failed to disrupt glucose sensing and neither could DVC lactate infusion recapitulate glucose effect. DVC oleic acid and glucose infusion failed to lower VLDL-TG secretion and glucose production in high-fat fed rats, while inhibiting DVC farnesoid X receptor enhanced oleic acid but not glucose sensing. Thus, an impairment of DVC nutrient sensing may lead to the disruption of lipid and glucose homeostasis in metabolic syndrome.

INTRODUCTION

Metabolic syndrome is characterized by hyperlipidemia and hyperglycemia due partly to increased hepatic secretion of triglyceride-rich very-low-density lipoprotein (VLDL-TG) and glucose production (DeFronzo et al., 1989; Reaven et al., 1993; Sherling et al., 2017). In recent decades, studies documented the role of the central nervous system (CNS) in lipid and glucose homeostasis (Grayson et al., 2013; Nogueiras et al., 2010; Schwartz et al., 2013; Taher et al., 2017).

The hypothalamus regulates lipid and glucose profiles in response to insulin (Koch et al., 2008; Obici et al., 2002a; Scherer et al., 2016; Yue and Lam, 2012), leptin (Buettner et al., 2008; Liu et al., 1998; Morton and Schwartz, 2011), glucagon-like peptide-1 (GLP-1) (Sandoval et al., 2008; Taher et al., 2014), ghrelin (Stark et al., 2015; Theander-Carrillo et al., 2006), melanocortin (Leckstrom et al., 2011; Nogueiras et al., 2007; Obici et al., 2001), and fibroblast grow factors (Morton et al., 2013; Scarlett et al., 2019) in rodents. In parallel, activation of ATP-sensitive potassium (K_{ATP}) channels in the hypothalamus and dorsal vagal complex (DVC) is sufficient and required for insulin to suppress glucose production in rodents during the pancreatic-euglycemic clamps (Filippi et al., 2012; Pocai et al., 2005), while oral K_{ATP} channel activator diazoxide intake in humans suppresses glucose production with the CNS implicated as the site of action (Kishore et al., 2011). Further, intranasal insulin delivery in healthy humans increases insulin sensitivity and lowers glucose production independent of changes in circulating insulin levels (Dash et al., 2015; Heni et al., 2014), while genome-wide association study-identified gene *DUSP8* mediates hypothalamic insulin sensitivity in both rodents and humans (Schriever et al., 2020). The relative contribution of the hypothalamus vs. DVC in glucose homeostasis remains unknown.

The hypothalamus detects amino acids (Arrieta-Cruz et al., 2013; Su et al., 2012), oleic acids (Obici et al., 2002b; Pocai et al., 2006), and glucose (Lam et al., 2005a) to regulate hepatic glucose production. Hypothalamic K_{ATP} channels is required for glucose sensing (Lam et al., 2005a), and such a finding was recently replicated in rodents as well as implicated in humans (Carey et al., 2020). Further, genetic manipulation of glucose-sensitive hypothalamic pro-opiomelanocortin neurons impairs glucose tolerance (Parton et al.,

[1]Department of Physiology, University of Toronto, Toronto, ON M5S 1A8, Canada

[2]Toronto General Hospital Research Institute, UHN, MaRS Center, TMDT 101 College Street, 10-705, Toronto, ON M5G 1L7, Canada

[3]Medical Research Institute, Kangbuk Samsung Hospital, Sungkyunkwan University School of Medicine, Seoul 03181, Republic of Korea

[4]Department of Physiology, University of Alberta, Edmonton, AB T6G 2H7, Canada

[5]Department of Medicine, University of Toronto, Toronto, ON M5S 1A8, Canada

[6]Banting and Best Diabetes Centre, University of Toronto, Toronto, ON M5G 2C4, Canada

[7]Lead contact

*Correspondence: tony.lam@uhnresearch.ca

https://doi.org/10.1016/j.isci.2021.102366

2007), while hypothalamic infusion of glucose blunts counter-regulation during hypoglycemia (Borg et al., 1997; Frizzell et al., 1993). Hypothalamic nutrient sensing regulates lipid homeostasis as well since hypothalamic infusion of oleic acid and glucose suppresses VLDL-TG secretion (Lam et al., 2007; Yue et al., 2015). As hypothalamic oleic acid infusion lowers feeding and neuropeptide Y expression (Obici et al., 2002b), hypothalamic infusion of neuropeptide Y exerts the opposing effect as oleic acid in elevating VLDL-TG secretion (Bruinstroop et al., 2012; Stafford et al., 2008). To date, hypothalamic nutrient sensing mechanism remains elusive.

Glucose transporter-1 in the hypothalamic glial cells and hypothalamic lactate dehydrogenase (LDH)-dependent metabolism as well as glucose/lactate-responsive neurons mediate glucose sensing (Chari et al., 2011; Lam et al., 2005a; Yoon and Diano, 2021), while leptin enhances LDH-dependent hypothalamic glucose sensing mechanism to regulate glucose production as well in high fat (HF) rats (Abraham et al., 2018). On the other hand, hypothalamic esterification of long-chain fatty acids via long-chain acyl-CoA synthase (ACSL) is required for oleic acid sensing (Lam et al., 2005b). NMDA receptor-mediated transmission in the DVC relays both hypothalamic glucose and oleic acid sensing mechanism to lower hepatic glucose production and VLDL-TG secretion, respectively (Lam et al., 2011; Yue et al., 2015). DVC is a highly permeable region in the brainstem which contains a circumventricular organ termed the area postrema as well as the nucleus of the solitary tract and the dorsal motor nucleus of the vagus. DVC relays signals from the gut and midbrain to facilitate energy and nutrient homeostasis (Blouet et al., 2009; Grill and Hayes, 2012; Lam et al., 2011; Waise et al., 2018; Wang et al., 2008; Yue et al., 2015) but also senses insulin (Filippi et al., 2012, 2014, 2017; Patel et al., 2021; Zhang et al., 2020), glucagon (LaPierre et al., 2015), leptin (Hayes et al., 2010; Kanoski et al., 2012), and GLP-1 (Alhadeff et al., 2017; Hayes et al., 2008, 2009) to regulate metabolism. DVC senses amino acid to lower food intake (Blouet and Schwartz, 2012), while DVC glucoprivation activates counter-regulation and increases food intake as well (Andrew et al., 2007; Ritter et al., 2000). Indeed, DVC contains glucose-sensitive neurons (Balfour et al., 2006; Mizuno and Oomura, 1984) and astrocytes that increase calcium influx in response to glucoprivation (McDougal et al., 2013). Given that ACSL (Bauer et al., 2018a; Briski et al., 2017) and LDH (Laughton et al., 2000) are expressed in the DVC, we evaluated whether ACSL or LDH-dependent lactate metabolism is necessary for fatty acid and glucose sensing.

Rats fed with a HF lard oil-enriched diet for 3 days develop insulin resistance, hyperlipidemia, and elevated hepatic secretion of VLDL-TG independent of obesity (Abraham et al., 2018; Chari et al., 2008; Côté et al., 2015; Scherer et al., 2012; Wang et al., 2001; Yue et al., 2012, 2015). Short-term HF feeding increases inflammation and endoplasmic reticulum stress in the hypothalamus (Ono et al., 2008; Thaler et al., 2012) and DVC (Filippi et al., 2017), resulting in insulin resistance. The ability of insulin to suppress glucose production is also blunted in lean and obese women after 3d HF feeding (Cornier et al., 2006) and in healthy men after 5 d of HF feeding (Brøns et al., 2009). While hypothalamic nutrient sensing is disrupted in HF feeding (Abraham et al., 2018; Yue et al., 2015), the impact on DVC nutrient sensing remains unknown. Further, inhibition of DVC farnesoid X receptor (FXR) enhances insulin sensitivity (Zhang et al., 2020) and in the small intestine mediates oleic acids and metformin to regulate glucose homeostasis (Bauer et al., 2018a; Jiang et al., 2015; Sun et al., 2018). Thus, we first tested whether DVC detects nutrients to regulate hepatic nutrient metabolism. Second, we evaluated the role of ACSL- and LDH-mediated DVC nutrient metabolism. Finally, we evaluated DVC nutrient sensing and the role of FXR in HF-fed rats. Our findings have revealed that infusion of nutrients into the DVC impacts systemic nutrient metabolism in rats.

RESULTS

Oleic acid sensing in the DVC lowers VLDL-TG secretion via ACSL

To examine whether the DVC senses oleic acids to regulate lipid homeostasis via a negative feedback pathway in rats *in vivo*, we have directly infused 1 mM oleic acid into DVC of 8-10 hr fasted, healthy, unrestrained rats at 0.33 ul/hr for 160 min (Figures 1A, 1B, S1A, and S1B). The dosage of oleic acids infusion selected has been documented to lower hepatic VLDL-TG secretion when infused into the hypothalamus of rats (Yue et al., 2015). To evaluate changes in lipid metabolism, lipoprotein lipase was inhibited either by chemical inhibitor tyloxapol or poloxamer to prevent VLDL-TG clearance in the plasma (Figure 1B). Then, plasma triglyceride (TG) accumulation was measured as a function of time to determine the hepatic secretion rate of VLDL-TG. Chylomicrons do not contribute to the rise of plasma TG in rats fasted for at least for 4 hr (Stafford et al., 2008). Herein, we have first found that plasma TG levels and the rate of VLDL-TG secretion of rats given DVC vehicle (2.6% cyclodextrin) infusion with tyloxapol injection were comparable with those of previous studies (Yue et al., 2012, 2015) (Figures 1C and 1D). Importantly, oleic acid administration into the DVC

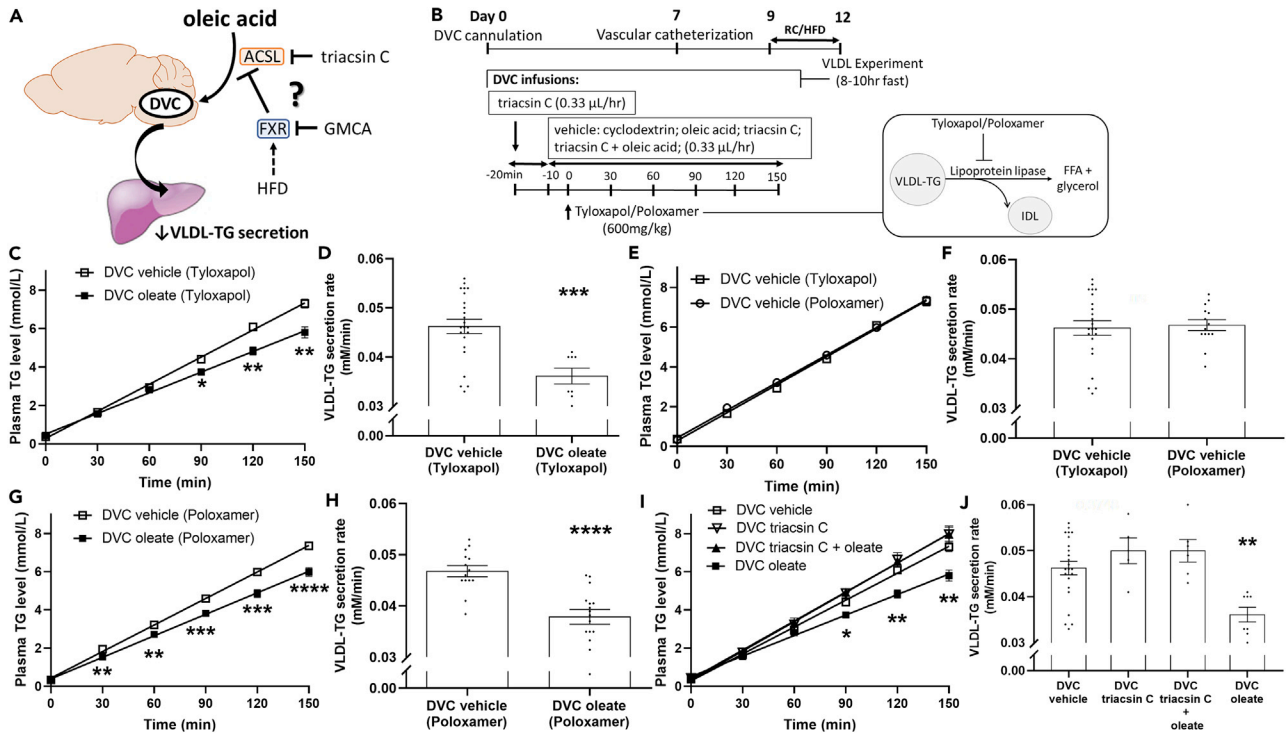

Figure 1. Oleic acid sensing in the DVC lowers VLDL-TG secretion via ACSL

(A) Schematic representation of working hypothesis.

(B) Experimental protocol for VLDL-TG assessments. IDL: intermediate-density lipoprotein; FFA: free fatty acid.

(C and D) (C) Plasma TG levels and (D) VLDL-TG secretion rate of tyloxapol-infused rats with DVC vehicle or oleate infusions (n = 23, 8).

(E and F) (E) Plasma TG level and (F) VLDL-TG secretion rate of tyloxapol- or poloxamer-infused rats with DVC vehicle infusions (n = 23, 14).

(G and H) (G) Plasma TG levels and (H) VLDL-TG secretion rate of poloxamer-infused rats with DVC vehicle or oleate infusions (n = 14, 16).

(I and J) (I) Plasma TG levels and (J) VLDL-TG secretion rate of rats receiving vehicle, ACSL inhibitor triacsin C, triacsin C + oleate, or oleate (n = 23, 5, 6, 8).

*p < 0.05, **p < 0.01, ***p < 0.001, ****p < 0.0001 vs. all other group(s) as determined by unpaired t test or one-way analysis of variance (ANOVA) with Tukey's test where appropriate. Data are presented as mean ± standard error of the mean.

decreased the rise in plasma TG levels in lipoprotein lipase-inhibited rats (Figure 1C) at comparable body weights to vehicle (0.321 ± 0.007 kg vs. vehicle 0.318 ± 0.003 kg; n = 23, 8). This lipid-lowering effect by oleic acid infusion into the DVC corresponded to a reduction in VLDL-TG secretion rate (Figure 1D).

An alternative lipoprotein lipase inhibitor, poloxamer, that is much easier to dissolve than tyloxapol was also used. In rats with comparable body weight (tyloxapol 0.321 ± 0.007 kg vs. poloxamer 0.329 ± 0.005 kg; n = 23, 14), plasma TG level and VLDL-TG secretion rate of DVC vehicle-infused rats injected with poloxamer vs. tyloxapol had identical plasma TG levels and VLDL-TG accumulation rate (Figures 1E and 1F). Importantly, DVC oleic acid vs. vehicle administration was equally effective in lowering plasma TG levels and the rate of VLDL-TG secretion in poloxamer-injected rats (Figures 1G and 1H) at comparable body weight and food intake (Table 1). Thus, oleic acid infusion into the DVC lowers VLDL-TG secretion via the use of two alternative assessment methods.

Oleic acid sensing in the upper small intestine and hypothalamus requires a long-chain acyl-CoA synthetase to esterify long-chain fatty acids to regulate hepatic glucose production and glucose homeostasis (Bauer et al., 2018a; Lam et al., 2005b; Wang et al., 2008). To begin delineating the mechanism underlying DVC oleic acid sensing in lipid homeostasis, we have infused triacsin C, a long-chain acyl-CoA synthetase inhibitor, to evaluate whether ACSL is required (Figures 1A and 1B). DVC administration of triacsin C alone vs. vehicle had no effect on VLDL-TG profiles in tyloxapol-injected rats at comparable weight (Figures 1I and 1J and Table 1). However, co-infusion of triacsin C with oleic acid into the DVC negated the ability of oleic acid infusion to lower plasma TG levels and VLDL-TG secretion rate (Figures 1I and 1J). Thus, long-chain acyl-CoA synthetase in the DVC is necessary for oleic acid sensing to lower hepatic VLDL-TG secretion in healthy rats.

Table 1. Food intake and body weight of rats which underwent VLDL (poloxamer-infused) and clamp experiments

	3d Cumulative food intake (kcal)	Body weight (kg)
VLDL		
RC + DVC vehicle (cyclodextrin) (n = 14)	164.0 ± 5.6	0.329 ± 0.005
RC + DVC oleic acid (n = 16)	183.3 ± 5.0	0.336 ± 0.004
RC + DVC vehicle (DMSO) + IV saline (n = 7)	159.0 ± 9.6	0.334 ± 0.009
RC + DVC vehicle (DMSO) +IV IH (n = 7)	172.3 ± 6.9	0.332 ± 0.006
RC + DVC triacsin C + IV IH (n = 6)	157.1 ± 13	0.327 ± 0.010
HFD + DVC vehicle (cyclodextrin) (n = 13)	235.8 ± 3.9[a]	0.340 ± 0.003
HFD + DVC oleic acid (n = 10)	232.1 ± 3.2[a]	0.342 ± 0.005
HFD + DVC GMCA (n = 6)	243.1 ± 6.7[a]	0.338 ± 0.004
HFD + DVC GMCA + oleic acid (n = 5)	232.4 ± 4.7[a]	0.359 ± 0.007
Pancreatic clamps		
Euglycemic clamps		
RC + DVC saline (n = 9)	185.6 ± 7.8	0.323 ± 0.009
RC + DVC glucose (n = 24)	171.0 ± 8.7	0.324 ± 0.004
RC + DVC lactate (n = 14)	174.7 ± 15	0.322 ± 0.006
RC + DVC oxamate + glucose (n = 5)	164.3 ± 12	0.321 ± 0.008
Hyperglycemic Clamp		
RC (n = 7)	150.6 ± 13	0.331 ± 0.007
HFD + DVC saline (n = 11)	230.1 ± 15[a]	0.334 ± 0.009
HFD + DVC glucose (n = 14)	232.5 ± 9.8[a]	0.338 ± 0.006
HFD + DVC GMCA (n = 6)	252.9 ± 13[a]	0.340 ± 0.006
HFD + DVC GMCA + glucose (n = 7)	238.5 ± 14[a]	0.339 ± 0.011

[a]$p < 0.05$ vs. RC groups as determined one-way ANOVA with Tukey's test. Data are presented as mean ± standard error of the mean for 3d cumulative food intake and body weight obtained prior to the VLDL or clamp studies.

DVC sensing of circulating lipid is required for VLDL-TG regulation

To begin examining the physiological relevance of DVC oleic acid sensing in whole-body lipid homeostasis, we infused 20% intralipid with heparin intravenously (IV IH) to elevate circulating free fatty acids levels (Chapados et al., 2009; Lam et al., 2003; Zhang et al., 2004) at a dose that would activate hypothalamic lipid sensing (Lam et al., 2005b). Concurrently, we infused triacsin C into the DVC at a dose that will negate DVC oleic acid sensing (Figures 1I and 1J) to evaluate whether VLDL-TG secretion in responses to IV IH would be disrupted (Figures 2A and 2B). We first detected a rise in plasma TG levels after 180 min of IV IH infusion (IV IH + DVC vehicle: −180 min = 0.33 ± 0.02 vs. 0 min = 0.86 ± 0.10 mM, $p < 0.001$; IV IH + DVC triacsin C: −180 min = 0.31 ± 0.03 vs. 0 min = 0.89 ± 0.06 mM, $p < 0.0001$). Rats that received intravenous (IV) saline for 180 min did not present any difference in plasma TG levels (−180 min = 0.368 ± 0.04, 0 min = 0.384 ± 0.03 mM). Consistent with previous studies (Chapados et al., 2009; Zhang et al., 2004), IV IH + DVC vehicle vs. IV saline + DVC vehicle infusion increased VLDL-TG secretion 45 min after poloxamer injection (Figures 2C and 2D). Importantly, disruption of lipid sensing mechanism in the DVC by DVC triacsin C infusion in the presence of IV IH infusion resulted in higher plasma TG levels and VLDL-TG secretion as compared to rats receiving IV IH + DVC vehicle infusion (Figures 2C and 2D). These results demonstrate that DVC senses circulating lipids to regulate systemic lipid homeostasis during a physiological increase of plasma lipid levels in rats.

Glucose sensing in the DVC suppresses glucose production independent of lactate metabolism

To examine whether DVC detects a rise in glucose to regulate glucose homeostasis via a negative feedback pathway in rats *in vivo*, we have administered 2 mM glucose vs. saline into the DVC at a dosage that will lower hepatic glucose production when administered to the hypothalamus (Chari et al., 2011; Lam et al., 2005a; Yang et al., 2010) and performed the pancreatic (basal insulin)-euglycemic clamps to evaluate changes in glucose kinetics in steady state (Figure 3A). Rats were comparable in weight and food intake (Table 1) and were

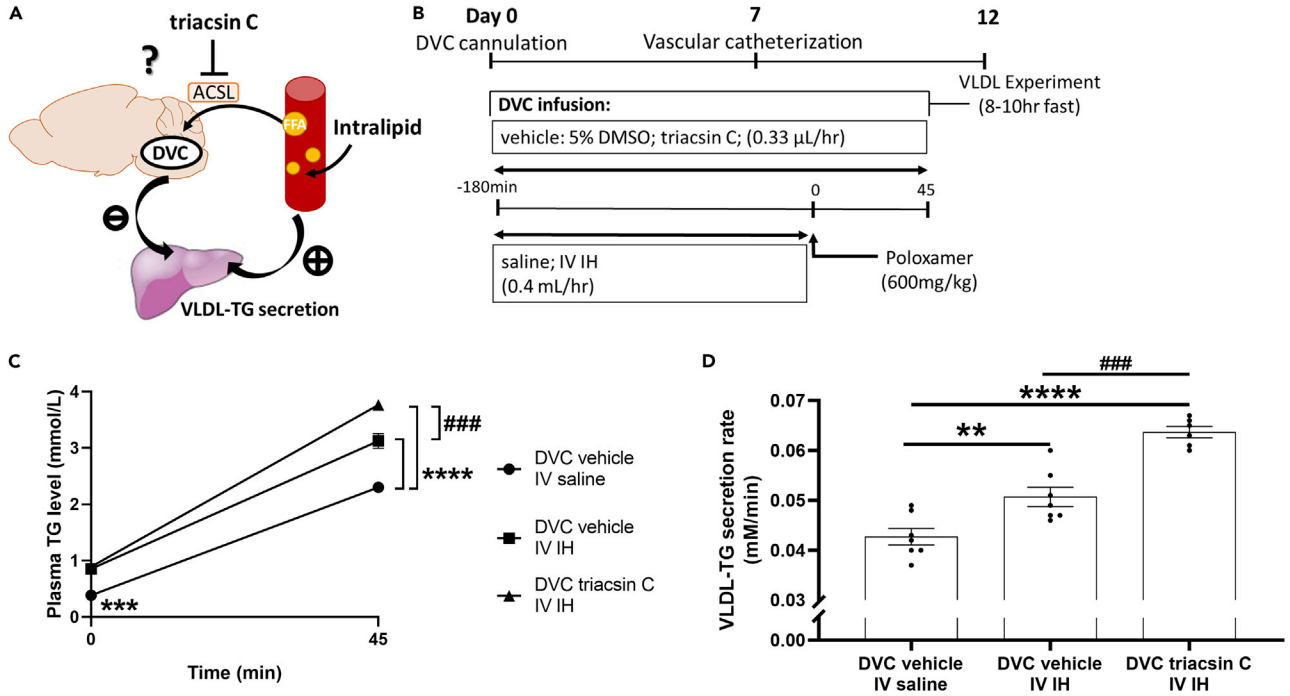

Figure 2. DVC sensing of circulating lipid is required for VLDL-TG regulation

(A) Schematic representation of working hypothesis.

(B) Experimental protocol for intravenous intralipid + DVC infusion followed by VLDL-TG assessments.

(C and D) (C) Plasma TG levels and (D) VLDL-TG secretion rate of poloxamer-infused rats with DVC vehicle + intravenous (IV) saline, DVC vehicle + IV intralipid + heparin (IH), or DVC triacsin C + IV IH infusions (n = 7, 7, 6).

**p < 0.01, ***p < 0.001, ****p < 0.0001, and ###p < 0.001 as determined by one-way ANOVA with Tukey's test. Data are presented as mean ± standard error of the mean.

randomly selected to receive DVC saline or glucose infusions. DVC glucose vs. saline infusion for 210 min increased the exogenous glucose infusion (Figure 3B) required to maintain euglycemia (Table 2) during the clamps. Analysis using the tracer dilution methodology revealed that the increased demand of glucose infusion was due to a suppression of glucose production (Figures 3C and 3D) and not an increase in glucose uptake (Figure 3E). Thus, glucose infusion into the DVC lowers glucose production in healthy rats.

To examine whether the astrocyte-neuronal lactate shuttle mediates glucose sensing in the DVC, we have first infused 5 mM lactate into the DVC of rats with comparable body weight and food intake to saline-infused rats (Table 1) to see whether it recapitulates the glucoregulatory effect of glucose. In contrast to the hypothalamus (Lam et al., 2005a; Yang et al., 2010), lactate infusion into the DVC failed to alter the glucose infusion rate and glucose production during the clamps (Figures 3F–3I and Table 2). To alternatively address for a potential glucoregulatory role of lactate metabolism in the DVC, we have co-infused the LDH inhibitor oxamate with glucose into the DVC at a dosage that will negate both lactate and glucose sensing in the hypothalamus (Abraham et al., 2018; Lam et al., 2005a). Co-infusion of oxamate with glucose into the DVC did not negate the ability of DVC glucose infusion to increase the glucose infusion rate (Figure 3F) required to maintain euglycemia (Table 2) during the clamps, which corresponded to a reduction in glucose production (Figures 3G and 3H) and not changes in glucose uptake (Figure 3I). Together, these results demonstrate that lactate is neither sufficient nor necessary for glucose infusion into the DVC to lower glucose production in healthy rats.

To verify that brain glucose infusion targeted the DVC, we independently infused radioactive tracer glucose through the DVC cannula at identical rate and duration as the DVC glucose infusion in clamps and collected DVC, mediobasal hypothalamus (MBH), and cortical tissue at the end. DVC infusion of radioactive glucose was found to selectively increase radioactivity in the DVC but not in the MBH and cortex of the same rats (Figure 4A). Next, to begin examining the physiological relevance of DVC glucose sensing,

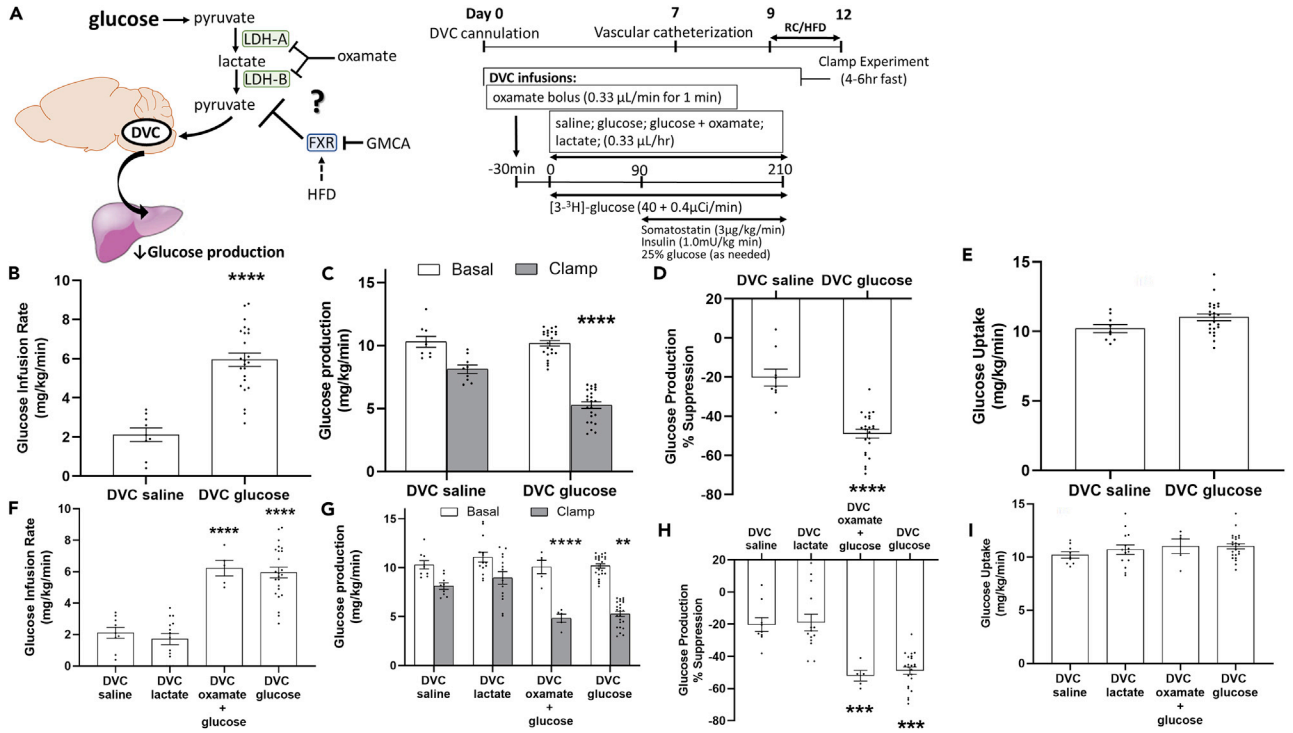

Figure 3. Glucose sensing in the DVC suppresses glucose production

(A) Schematic representation of working hypothesis and the pancreatic (basal insulin)-euglycemic clamp protocol.

(B–E) (B) Glucose infusion rate, (C) basal and clamp glucose production, (D) percentage suppression of clamp glucose production from basal, and (E) glucose uptake of rats with DVC saline or glucose infusions (n = 9, 24). ****p < 0.0001 vs. DVC saline as determined by unpaired t test.

(F–I) (F) Glucose infusion rate, (G) basal and clamp glucose production, (H) percentage suppression of clamp glucose production from basal, and (I) glucose uptake of rats with DVC saline, lactate, oxamate + glucose, or glucose infusions (n = 9, 14, 5, 24).

**p < 0.01, ***p < 0.001, ****p < 0.0001 vs. DVC saline and DVC lactate as determined by one-way ANOVA with Tukey's test. Data are presented as mean ± standard error of the mean.

we measured the glucose levels of DVC and MBH tissues obtained from rats that were clamped under euglycemic conditions receiving DVC saline or glucose and systemic hyperglycemic-pancreatic (basal insulin) clamp conditions. DVC glucose vs. saline infusion elevated glucose levels in the DVC by ~2 fold (Figure 4B) but not in the MBH (Figure 4C) while maintained under comparable plasma glucose levels (DVC glucose: 6.9 ± 0.33 vs. DVC saline: 6.7 ± 0.15 mM). We next performed systemic hyperglycemic-pancreatic clamps and raised and maintained plasma glucose levels by ~2.5 fold in rats (to 17.1 ± 0.49 mM, n = 7) by 2 hr that was previously documented to elevate hypothalamic glucose levels and activate hypothalamic glucose sensing to suppress glucose production (Lam et al., 2005a). We here first confirmed that MBH glucose levels were indeed raised (Figure 4C) by circulating hyperglycemia and found that DVC glucose levels (Figure 4B) were similarly elevated in the same rats. More importantly, the degree of elevation of DVC glucose levels incurred by the hyperglycemic clamps was comparable to that of the DVC glucose levels detected in response to DVC glucose infusion (Figure 4B). Together, these results further validate accurate placement and infusion of the brain cannula targeting the DVC and support that direct DVC glucose infusion elevates DVC glucose levels to a comparable extent as a physiological rise in plasma glucose concentration that would lower glucose production in healthy rats.

HF feeding disrupts oleic acid sensing in the DVC to suppress VLDL-TG secretion

To address for the pathological relevance of nutrient sensing in the DVC, we have fed surgically recovered rats with 3 days of high-fat diet (HFD) to see whether prior to the onset of obesity and in this short-term metabolically challenged model (Figures 1A, 1B, and 3A) DVC nutrient sensing remains intact. First, we have monitored the food intake and body weight of the HFD rats and confirmed that the rats became hyperphagic (Figure 5A), while no significant changes in body weight (Table 1) were observed. We have further detected a disruption of lipid homeostasis in these HF rats as HF vs. RC rats have elevated basal plasma TG levels (RC: 0.30 ± 0.02 mM

Table 2. Plasma glucose levels of rats during basal and clamp steady states of the pancreatic basal-insulin euglycemic clamps

	Plasma glucose (mM)	
	Basal (60-90 min)	Clamp (180-210 min)
RC + saline (n = 9)	7.6 ± 0.3	6.4 ± 0.4
RC + glucose (n = 24)	7.3 ± 0.1	7.1 ± 0.3
RC + lactate (n = 14)	7.2 ± 0.2	7.6 ± 0.3
RC + oxamate + glucose (n = 5)	7.1 ± 0.3	6.5 ± 0.3
HFD + saline (n = 11)	7.8 ± 0.1	7.3 ± 0.3
HFD + glucose (n = 14)	7.9 ± 0.2	6.7 ± 0.2
HFD + GMCA (n = 6)	8.2 ± 0.4	7.6 ± 0.3
HFD + GMCA + glucose (n = 7)	8.1 ± 0.1	7.7 ± 0.3

Data are presented as mean ± standard error of the mean.

vs. HFD 0.51 ± 0.03 mM, $p < 0.0001$) together with increased plasma TG levels and hepatic secretion of VLDL-TG in poloxamer-injected rats (Figures 5B and 5C). Importantly, oleic acid infusion into the DVC failed to lower plasma TG levels and hepatic secretion rate of VLDL-TG in poloxamer-injected HF rats as compared to the oleate effect that was seen in healthy rats (Figures 5B and 5C).

HF feeding disrupts glucose sensing in the DVC to suppress glucose production

Next, in an independent cohort of rats, we have first confirmed again that HF vs. RC rats were hyperphagic (Figure 6A) but with no changes in body weight (Table 1). We have then performed the pancreatic-euglycemic clamps in HF rats that received saline or glucose infusion into the DVC as in healthy rats (Figure 3A). In contrast to healthy rats, glucose administration into the DVC failed to increase glucose infusion rate (Figure 6B) during the clamps in maintaining euglycemia (Table 2). Further, glucose production and glucose uptake remained comparable among groups (Figures 6C–6E). Taken together, these results demonstrate that short-term HF feeding disrupts oleic acid and glucose infusion into the DVC to regulate hepatic VLDL-TG and glucose production.

FXR antagonism rescues oleic acid, but not glucose, sensing in the DVC

Next, we have tested whether inhibiting FXR via chemical inhibitor glyco-β-muricholic acid (GMCA) in the DVC could enhance oleic acid and glucose sensing to regulate lipid and glucose homeostasis in HF rats (Figures 1A and 3A). We have administered GMCA in the DVC of HF rats at the same dosage as previously described that would inhibit FXR signaling in the DVC of rats *in vivo* (Zhang et al., 2020) and first tested the response of DVC oleic acid sensing in VLDL-TG regulation (Figure 7A). In poloxamer-injected HF vs. RC rats that were hyperphagic (Figure 7B) but with comparable body weight (Table 1), GMCA administration in the DVC enhanced the ability of DVC oleic acid infusion to lower plasma TG levels and hepatic VLDL-TG secretion (Figures 7C and 7D) in HF rats to a similar level as seen in healthy rats (Figures 1G and 1H), while GMCA given at the current dosage into the DVC *per se* did not alter plasma TG levels and VLDL-TG secretion rate (Figures 7C and 7D) as compared to vehicle (Figures 5B and 5C).

Finally, we have administered GMCA in the DVC of HF rats at the same dosage as the VLDL-TG studies and tested the response of DVC glucose sensing during the clamps (Figure 7A). In HF vs. RC rats that were hyperphagic (Figure 7E) but with comparable body weight (Table 1), GMCA administration into the DVC failed to enhance the ability of DVC glucose infusion to regulate glucose metabolism in HF rats as compared to HF rats infused with DVC glucose (Figures 7F–7I), while DVC GMCA infusion alone did not alter glucose metabolism (Figures 7F–7I) as compared to saline (Figures 6B–6E). Taken together, these findings suggest that direct inhibition of FXR in the DVC of HF rats enhances oleic acid sensing to lower plasma TG and VLDL-TG secretion but fails to enhance DVC glucose sensing to regulate glucose metabolism.

DISCUSSION

The metabolic syndrome is associated with atherogenic dyslipidemia that includes hypertriglyceridemia and increased liver production of VLDL-TG, as well as hyperglycemia resulting from unsuppressed hepatic

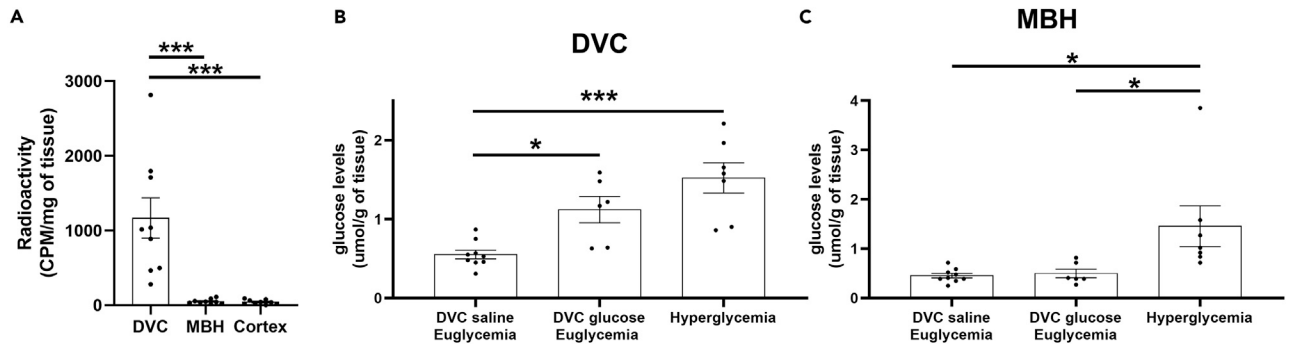

Figure 4. Infusion of glucose is localized in the DVC and elevates DVC glucose levels at a comparable extent as seen with systemic hyperglycemia

(A) Radioactivity level of DVC, MBH, and cortex tissue after DVC [3-^{3}H]-glucose infusion (n = 9).

(B and C) (B) DVC and (C) MBH tissue glucose levels after DVC saline-euglycemic, DVC glucose-euglycemic, or systemic hyperglycemic clamps (n = 9, 6, 7). *p < 0.05, ***p < 0.001 as determined by one-way ANOVA with Tukey's test. Data are presented as mean ± s.e.m.

glucose production (Sherling et al., 2017). Impaired lipid homeostasis, in turn, further exacerbates glucose dysregulation (Fu et al., 2012; Yue and Lam, 2012).

In this study, we have first demonstrated that ACSL is required for oleic acid infusion into the DVC to lower hepatic VLDL-TG secretion in rats. This is consistent with the fatty acid sensing mechanism observed for the upper small intestine (Bauer et al., 2018a; Wang et al., 2008) and the hypothalamus (Lam et al., 2005b). In addition, we have demonstrated that DVC lipid sensing is required for restraining and regulating VLDL-TG secretion in the presence of systemic elevated lipid levels. After short-term HF feeding, animals exhibit elevated basal plasma TG levels and concurrently impaired DVC lipid sensing. Together, these results suggest that failure of DVC lipid sensing to regulate VLDL-TG secretion may contribute to the dysregulation of lipid homeostasis in the short-term HF model and that the metabolic beneficial effects of acute CNS lipid sensing is offset by the long-term effect incurred by HF feeding. Future investigations are warranted to examine the physiological relevance of DVC oleic acid sensing and the associated impact in animal models with obesity and diabetes. In addition, in light of the fact that nutrient sensing in the hypothalamus and leptin action in the brain not only regulate hepatic VLDL-TG secretion but also subsequently affect hepatic TG levels in rodents (Lam et al., 2007; Hackl et al., 2019), further assessment on hepatic TG levels as well as lipogenesis is required in the current experimental settings.

HF not only negates fatty acid sensing in the small intestine (Bauer et al., 2018a; Cheung et al., 2009; Wang et al., 2008), hypothalamus (Yue et al., 2015), and as currently observed in DVC but also suppresses ACSL3 in the small intestine to disrupt fatty acid sensing (Bauer et al., 2018a). Given that ACSL3 is expressed in the DVC (Bauer et al., 2018a; Briski et al., 2017), we postulate that HF disrupts DVC oleic acid sensing via a reduction in ACSL3 expression. This is further supported by the fact that activation of upper small intestinal FXR in HF rats negates the ability of upper small intestinal healthy microbiome transplant to increase small intestinal ACSL3 expression and enhance fatty acid sensing glucoregulatory pathways (Bauer et al., 2018a), while direct inhibition of FXR in the DVC enhances oleic acid sensing to regulate hepatic VLDL-TG secretion in HF rats. In both the current and a previous study where direct infusion of glycine activated NMDA receptors in DVC to suppress hepatic VLDL-TG secretion, the first observance of lowered plasma TG levels was 30 min after lipid clearance is blocked (Yue et al., 2012). In the same study when hepatic vagotomy was performed, DVC glycine failed to alter VLDL-TG secretion. The ability of central secreted frizzled-related protein 5 and hypothalamic oleic acid sensing to suppress VLDL-TG secretion both require DVC NMDA signaling and hepatic vagal innervation (Li et al., 2020; Yue et al., 2015), together suggesting the possibility that DVC lipid sensing may modulate VLDL-TG secretion via NMDA receptors and the hepatic vagus. This warrants future investigations and may also give insights to the neuronal population mediating DVC oleic acid sensing.

On the other hand, DVC glucose sensing mechanism is in contrary to the hypothalamic mechanism (Abraham et al., 2018; Lam et al., 2005a) as lactate was neither sufficient nor necessary to lower glucose production. In addition, direct inhibition of FXR in the DVC failed to enhance glucose sensing in HF rats to lower glucose production. While increased lactate in the DVC blunts blood glucose level recovery during insulin-induced hypoglycemia and reduced lactate level by inhibition of monocarboxylate transporter

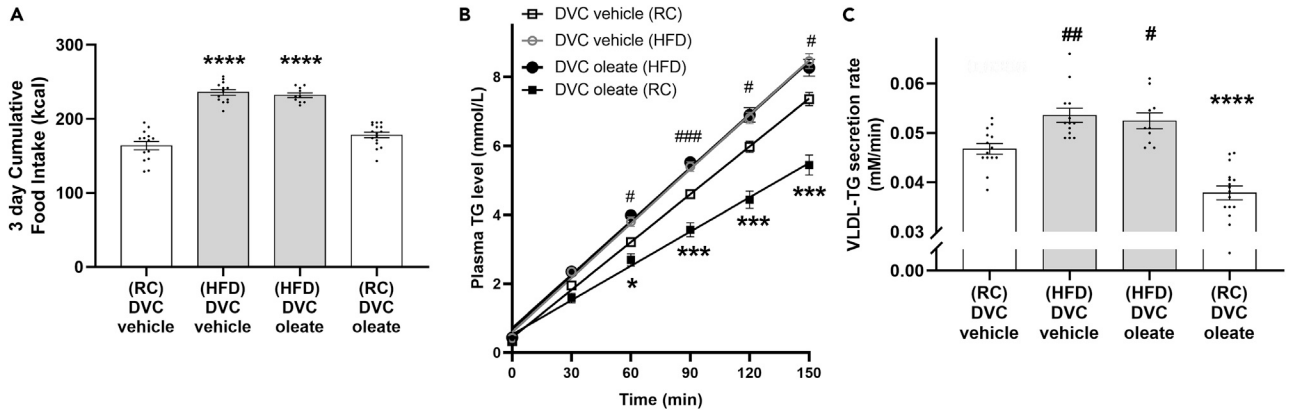

Figure 5. HF feeding disrupts oleic acid sensing in the DVC

(A) 3d cumulative food intake of DVC vehicle (RC), DVC vehicle (HFD), DVC oleate (HFD), or DVC oleate (RC) rats prior to experimentation (n = 14, 13, 10, 16). ****p < 0.0001 vs. RC groups.

(B and C) (B) Plasma TG levels and (C) VLDL-TG secretion rate of DVC vehicle (RC), DVC vehicle (HFD), DVC oleate (HFD), or DVC oleate (RC) infusion (n = 14, 13, 10, 16).

#p < 0.05, ###p < 0.001 for DVC vehicle/oleate (HFD) vs. RC groups. *p < 0.05, ***p < 0.001, ****p < 0.0001 for DVC vehicle (RC) vs. DVC oleate (RC) as determined by two-way ANOVA with Tukey's test. Data are presented as mean ± standard error of the mean.

increases blood glucose level (Gujar et al., 2014; Patil and Briski, 2005), it remains unknown why lactate infusion did not lower glucose production in the current pancreatic clamp setting where plasma glucose level was maintained at basal. The relevance of lactate metabolism lies in its potential to be converted to pyruvate and provide energy for the brain as supported by the astrocyte-neuron lactate shuttle hypothesis (Laughton et al., 2000; Pellerin and Magistretti, 1994), as well as studies demonstrating glucose metabolism-activated neurons also being responsive to lactate (Himmi et al., 2001; Yang et al., 1999). In our current findings, lactate did not mimic the effect of glucose even with substantial expression of LDH-B (converts lactate to pyruvate) detected in the DVC (Laughton et al., 2000), suggesting that the glucose sensing pathway we are examining may be independent of glucose metabolism (i.e. glycolysis). In support, glucose sensing in the small intestine does not require intestinal glucose metabolism to improve glucose tolerance but instead via the activation of sodium glucose cotransporter-1 and subsequent release of GLP-1 (Bauer et al., 2018b; Kuhre et al., 2015; Moriya et al., 2009). Consistently, the DVC contains glucose-sensitive neurons (Balfour et al., 2006), and glucose excites glucose-sensitive neurons via sodium glucose cotransporter-facilitated sodium entry (Gonzàlez et al., 2009; O'Malley et al., 2006). Although no study has directly identified sodium glucose transporter in the DVC, sodium glucose transporter is expressed at various regions of the brain (Poppe et al., 1997; Yu et al., 2013). In fact, a study infusing the sodium glucose cotransporter inhibitor phloridzin into the forth ventricle, which grants immediate exposure to the DVC, has demonstrated an elevation in food intake (Li et al., 2013). This finding may serve as an indicator of functional sodium glucose cotransporters in the region. Moreover, GLP-1-producing neurons are detected in the DVC, and when these neurons are activated in mice, it suppresses glucose production, promotes glucose tolerance, and improves hepatic insulin sensitivity (Shi et al., 2017). In support of a working hypothesis that glucose sensing in the DVC activates GLP-1-expressing neurons to facilitate glucose homeostasis, glucose has been documented to stimulate glutamate release (Boychuk et al., 2015; Roberts et al., 2017; Wan and Browning, 2008) and GLP-1-producing neurons have been characterized as glutamatergic (Zheng et al., 2015). Previous study has also demonstrated that the activation of NMDA receptors in the DVC lowers glucose production (Lam et al., 2010; Yue et al., 2016). Of note, GLP-1-producing neurons in the DVC may also mediate fatty acid sensing in regulating VLDL-TG secretion as fatty acid in the small intestine has been documented to stimulate GLP-1 release (Hirasawa et al., 2005; Iakoubov et al., 2007; Rocca et al., 2001), while activation of NMDA receptor in the DVC is sufficient and necessary to lower hepatic VLDL-TG secretion as well (Li et al., 2020; Yue et al., 2012, 2015). Nonetheless, future studies are required to further elucidate glucose and oleic acid sensing mechanism in the DVC, including the neuron type and neurocircuitry responsible as well as the time-dependent effect of nutrient sensing on VLDL-TG secretion and glucose production regulation, as a limitation of the current study is the incapacity to identify specific neurons within the DVC that are activated by nutrients to mediate the control of systemic metabolism.

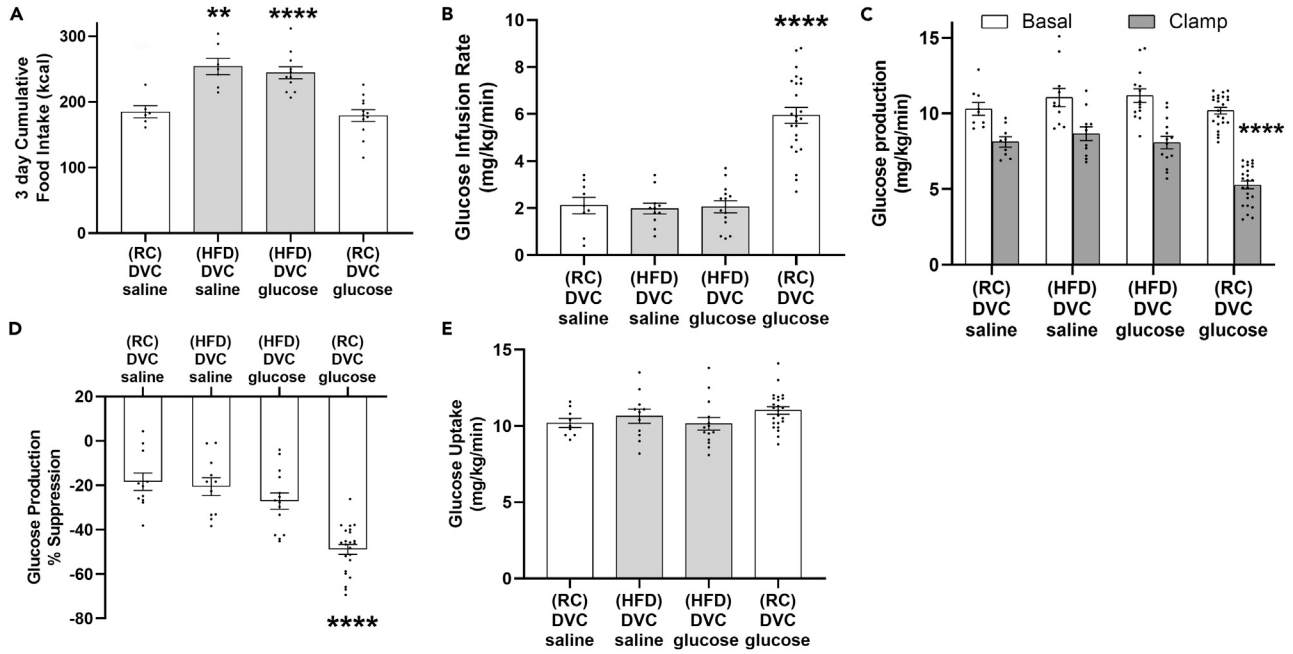

Figure 6. HF feeding disrupts glucose sensing in the DVC

(A) 3d cumulative food intake of DVC saline (RC), DVC saline (HFD), DVC glucose (HFD), or DVC glucose (RC) rats prior to experimentation (n = 9, 11, 14, 24). **p < 0.01, ****p < 0.0001 vs. RC groups.

(B–E) (B) Glucose infusion rate, (C) basal and clamp glucose production, (D) percentage suppression of clamp glucose production from basal, and (E) glucose uptake of DVC saline (RC), DVC saline (HFD), DVC glucose (HFD), or DVC glucose (RC) rats (n = 9, 11, 14, 24).

****p < 0.0001 vs. all other groups as determined by two-way ANOVA with Tukey's test. Data are presented as mean ± standard error of the mean.

It remains unknown why direct inhibition of FXR enhances fatty acid but not glucose sensing in the DVC of HF rats. One immediate postulation is that FXR inhibition may upregulate the expression of genes that mediate fatty acid sensing (i.e., ACSL3) but not glucose sensing (i.e., sodium glucose cotransporter-1) in the DVC. Indeed, HF feeding reduces ACSL3 expression in the upper small intestine, and this reduction is prevented by healthy microbiome transplant in an FXR-dependent manner (Bauer et al., 2018a). On the other hand, no study, to the best of our knowledge, has documented that FXR regulates SGLT expression.

We postulate that excess nutrient availability derived from the hyperphagic response induced by HF feeding may inhibit potential molecules within the CNS that would disrupt nutrient sensing. For instance, 3d of HF feeding reduces glucose transporter of the blood brain barrier and lowers brain glucose uptake (Jais et al., 2016). In an uncontrolled diabetic rat model with 24 hr sustained hyperglycaemia (excess glucose), hypothalamic glial cell glucose transporter-1 expression is suppressed, negating the ability of hypothalamic glucose sensing mechanism to elevate local glucose levels and suppress glucose production (Chari et al., 2011). Further, the ability of glucose to promote its own clearance, termed as glucose effectiveness, is lost in people with type 2 diabetes, while normalization of hyperglycaemia and/or hyperlipidemia restores glucose effectiveness (Hawkins et al., 2002). Nonetheless, it is to be acknowledged that a limitation of the current study is the assessment on DVC nutrient sensing resides only in the 3d HF-fed model. To address the effect of hyperphagia *per se* on DVC nutrient sensing, a model with high carbohydrate intake could also be tested. Future investigations are called for to investigate the contribution of DVC in regulation of lipid/glucose homeostasis in healthy state and whether restoration of DVC nutrient sensing pathways improves lipid/glucose homeostasis in not only diabetic and obese models.

In summary, we have unveiled fatty acid and glucose infusion into the DVC lower hepatic VLDL-TG secretion and glucose production in healthy but not HF rats and that direct inhibition of FXR in the DVC enhances fatty acid but not glucose sensing *in vivo*.

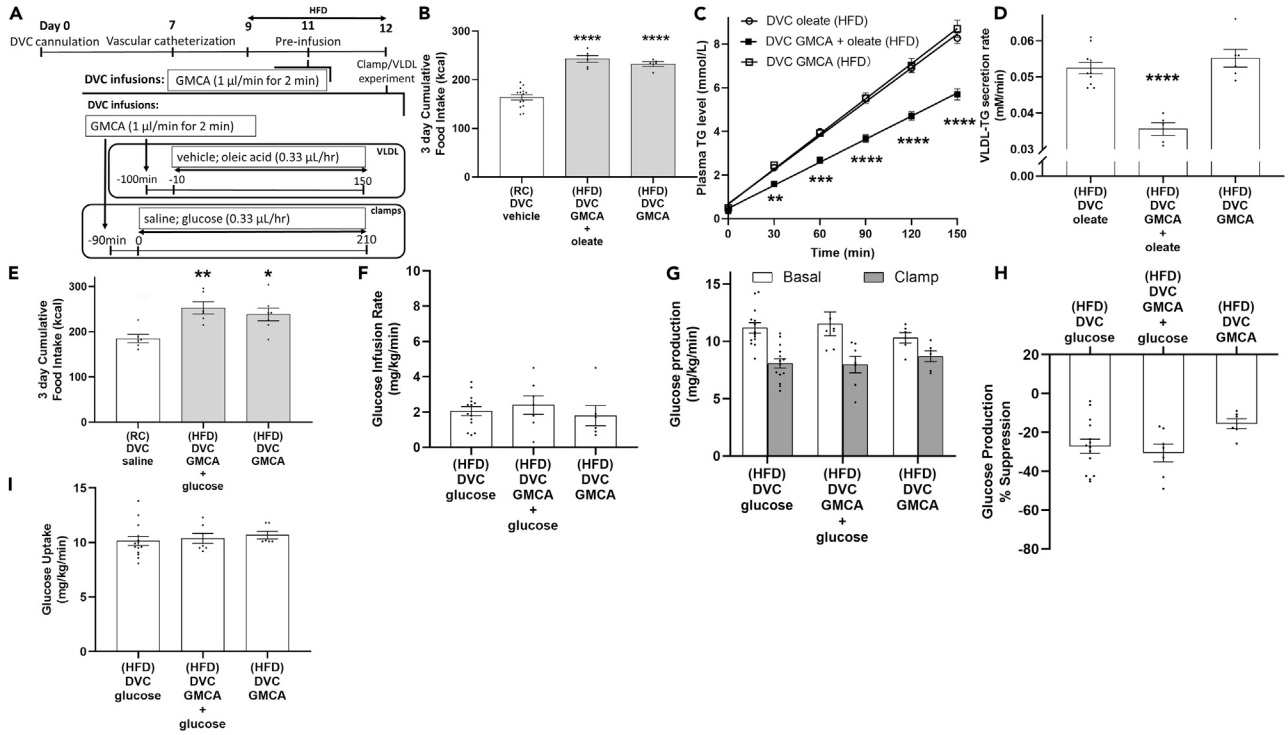

Figure 7. FXR antagonism rescues oleic acid, but not glucose, sensing in the DVC

(A) Schematic representation of the experimental protocol.

(B) 3d cumulative food intake of DVC vehicle (RC), DVC GMCA + oleate (HFD), or DVC GMCA (HFD) rats prior to experimentation (n = 14, 5, 6). ****p < 0.0001 vs. DVC vehicle (RC).

(C and D) (C) Plasma TG levels and (D) VLDL-TG secretion rate of HFD rats with DVC oleate, GMCA + oleate, or GMCA infusions (n = 10, 5, 6). **p < 0.01, ***p < 0.001, ****p < 0.0001 vs. all groups.

(E) 3d cumulative food intake of DVC saline (RC), DVC GMCA + glucose (HFD), or DVC GMCA (HFD) rats prior to experimentation (n = 9, 7, 6). *p < 0.05, **p < 0.01 vs. DVC saline (RC) as determined by one-way ANOVA with Tukey's test.

(F–I) (F) Glucose infusion rate, (G) basal and clamp glucose production, (H) percentage suppression of clamp glucose production from basal, and (I) glucose uptake of HFD animals with DVC glucose, GMCA + glucose, or GMCA infusions (n = 14, 7, 6). Data are presented as mean ± standard error of the mean.

Limitations of study

The current study did not address the metabolic impact of nutrient sensing in the DVC of male and female rodents with obesity and/or diabetes and neither identify specific neuron(s) in the DVC that mediate nutrient sensing to regulate hepatic nutrient metabolism. The downstream mechanism of glucose sensing as well as the inability of FXR inhibition to enhance glucose sensing in the DVC remains unknown.

Resource availability

Lead contact

Further information and requests for resources and reagents should be directed to and will be fulfilled by the lead contact, Tony K.T. Lam (tony.lam@uhnresearch.ca).

Materials availability

This study did not generate new unique reagents.

Data and code availability

This study did not use any unpublished custom code, software, or algorithm that is central to supporting the main claims of the paper.

METHODS

All methods can be found in the accompanying transparent methods supplemental file.

SUPPLEMENTAL INFORMATION

Supplemental information can be found online at https://doi.org/10.1016/j.isci.2021.102366.

ACKNOWLEDGMENTS

R.J.W.L. is supported by a Banting and Best Diabetes Center (BBDC) graduate scholarship. S-Y. Z is supported by a BBDC post-doctoral fellowship. Y-M. L. is supported by a BBDC-Kangbuk Samsung fellowship. This study was supported by a Canadian Institutes of Health Research Foundation Grant to T.K.T.L. (FDN-143204). J.T.Y.Y holds the Diabetes Canada Scholar (SC-5-16-5060-JY) and Tier 2 Canada Research Chair in Brain Regulation of Metabolism. T.K.T.L. holds the John Kitson McIvor (1915-1942) Endowed Chair in Diabetes Research and the Tier 1 Canada Research Chair in Diabetes and Obesity at the Toronto General Hospital Research Institute and the University of Toronto.

AUTHOR CONTRIBUTIONS

R.J.W.L. conducted and designed the experiments, performed the data analyses, and wrote the manuscript. B.B. conducted the experiments, and M.A.A., B.W., S-Y.Z., and Y.-M.L. assisted with experiments. J.T.Y.Y. assisted with experiments and experimental design. T.K.T.L. supervised the project, designed the experiments, and edited the manuscript.

DECLARATION OF INTERESTS

The authors declare no conflict of interest.

Received: October 20, 2020
Revised: February 8, 2021
Accepted: March 24, 2021
Published: April 23, 2021

REFERENCES

Abraham, M.A., Rasti, M., Bauer, P.V., and Lam, T.K.T. (2018). Leptin enhances hypothalamic lactate dehydrogenase A (LDHA)-dependent glucose sensing to lower glucose production in high-fat-fed rats. J. Biol. Chem. *293*, 4159–4166.

Alhadeff, A.L., Mergler, B.D., Zimmer, D.J., Turner, C.A., Reiner, D.J., Schmidt, H.D., Grill, H.J., and Hayes, M.R. (2017). Endogenous glucagon-like peptide-1 receptor signaling in the nucleus tractus solitarius is required for food intake control. Neuropsychopharmacology *42*, 1471–1479.

Andrew, S.F., Dinh, T.T., and Ritter, S. (2007). Localized glucoprivation of hindbrain sites elicits corticosterone and glucagon secretion. Am. J. Physiol. Regul. Integr. Comp. Physiol. *292*, R1792–R1798.

Arrieta-Cruz, I., Su, Y., Knight, C.M., Lam, T.K.T., and Gutiérrez-Juárez, R. (2013). Evidence for a role of proline and hypothalamic astrocytes in the regulation of glucose metabolism in rats. Diabetes *62*, 1152–1158.

Balfour, R.H., Hansen, A.M.K., and Trapp, S. (2006). Neuronal responses to transient hypoglycaemia in the dorsal vagal complex of the rat brainstem. J. Physiol. *570*, 469–484.

Bauer, P.V., Duca, F.A., Waise, T.M.Z., Dranse, H.J., Rasmussen, B.A., Puri, A., Rasti, M., O'Brien, C.A., and Lam, T.K.T. (2018a). Lactobacillus gasseri in the upper small intestine impacts an ACSL3-dependent fatty acid-sensing pathway regulating whole-body glucose homeostasis. Cell Metab. *27*, 572–587.e6.

Bauer, P.V., Duca, F.A., Waise, T.M.Z., Rasmussen, B.A., Abraham, M.A., Dranse, H.J., Puri, A., O'Brien, C.A., and Lam, T.K.T. (2018b). Metformin alters upper small intestinal microbiota that impact a glucose-SGLT1-sensing glucoregulatory pathway. Cell Metab. *27*, 101–117.e5.

Blouet, C., and Schwartz, G.J. (2012). Brainstem nutrient sensing in the nucleus of the solitary tract inhibits feeding. Cell Metab. *16*, 579–587.

Blouet, C., Jo, Y.-H., Li, X., and Schwartz, G.J. (2009). Mediobasal hypothalamic leucine sensing regulates food intake through activation of a hypothalamus-brainstem circuit. J. Neurosci. *29*, 8302–8311.

Borg, M.A., Sherwin, R.S., Borg, W.P., Tamborlane, W.V., and Shulman, G.I. (1997). Local ventromedial hypothalamus glucose perfusion blocks counterregulation during systemic hypoglycemia in awake rats. J. Clin. Invest. *99*, 361–365.

Boychuk, C.R., Gyarmati, P., Xu, H., and Smith, B.N. (2015). Glucose sensing by GABAergic neurons in the mouse nucleus tractus solitarii. J. Neurophysiol. *114*, 999–1007.

Briski, K.P., Alenazi, F.S.H., Shakya, M., and Sylvester, P.W. (2017). Hindbrain A2 noradrenergic neuron adenosine 5′-monophosphate-activated protein kinase activation, upstream kinase/phosphorylase protein expression, and receptivity to hormone and fuel reporters of short-term food deprivation are regulated by estradiol. J. Neurosci. Res. *95*, 1427–1437.

Brøns, C., Jensen, C.B., Storgaard, H., Hiscock, N.J., White, A., Appel, J.S., Jacobsen, S., Nilsson, E., Larsen, C.M., Astrup, A., et al. (2009). Impact of short-term high-fat feeding on glucose and insulin metabolism in young healthy men. J. Physiol. *587*, 2387–2397.

Bruinstroop, E., Pei, L., Ackermans, M.T., Foppen, E., Borgers, A.J., Kwakkel, J., Alkemade, A., Fliers, E., and Kalsbeek, A. (2012). Hypothalamic neuropeptide Y (NPY) controls hepatic VLDL-triglyceride secretion in rats via the sympathetic nervous system. Diabetes *61*, 1043–1050.

Buettner, C., Muse, E.D., Cheng, A., Chen, L., Scherer, T., Pocai, A., Su, K., Cheng, B., Li, X., Harvey-White, J., et al. (2008). Leptin controls adipose tissue lipogenesis via central, STAT3-independent mechanisms. Nat. Med. *14*, 667–675.

Carey, M., Lontchi-Yimagou, E., Mitchell, W., Reda, S., Zhang, K., Kehlenbrink, S., Koppaka, S., Maginley, S.R., Aleksic, S., Bhansali, S., et al. (2020). Central KATP channels modulate glucose effectiveness in humans and rodents. Diabetes *69*, 1140–1148.

Chapados, N.A., Seelaender, M., Levy, E., and Lavoie, J.M. (2009). Effects of exercise training on hepatic microsomal triglyceride transfer protein content in rats. Horm. Metab. Res. *41*, 287–293.

Chari, M., Lam, C.K.L., Wang, P.Y.T., and Lam, T.K.T. (2008). Activation of central lactate

metabolism lowers glucose production in uncontrolled diabetes and diet-induced insulin resistance. Diabetes *57*, 836–840.

Chari, M., Yang, C.S., Lam, C.K.L., Lee, K., Mighiu, P., Kokorovic, A., Cheung, G.W.C., Lai, T.Y.Y., Wang, P.Y.T., and Lam, T.K.T. (2011). Glucose transporter-1 in the hypothalamic glial cells mediates glucose sensing to regulate glucose production in vivo. Diabetes *60*, 1901–1906.

Cheung, G.W.C., Kokorovic, A., Lam, C.K.L., Chari, M., and Lam, T.K.T. (2009). Intestinal cholecystokinin controls glucose production through a neuronal network. Cell Metab. *10*, 99–109.

Cornier, M.-A., Bergman, B.C., and Bessesen, D.H. (2006). The effects of short-term overfeeding on insulin action in lean and reduced-obese individuals. Metab. Clin. Exp. *55*, 1207–1214.

Côté, C.D., Rasmussen, B.A., Duca, F.A., Zadeh-Tahmasebi, M., Baur, J.A., Daljeet, M., Breen, D.M., Filippi, B.M., and Lam, T.K.T. (2015). Resveratrol activates duodenal Sirt1 to reverse insulin resistance in rats through a neuronal network. Nat. Med. *21*, 498–505.

Dash, S., Xiao, C., Morgantini, C., Koulajian, K., and Lewis, G.F. (2015). Intranasal insulin suppresses endogenous glucose production in humans compared with placebo in the presence of similar venous insulin concentrations. Diabetes *64*, 766–774.

DeFronzo, R.A., Ferrannini, E., and Simonson, D.C. (1989). Fasting hyperglycemia in non-insulin-dependent diabetes mellitus: contributions of excessive hepatic glucose production and impaired tissue glucose uptake. Metab. Clin. Exp. *38*, 387–395.

Filippi, B.M., Yang, C.S., Tang, C., and Lam, T.K.T. (2012). Insulin activates Erk1/2 signaling in the dorsal vagal complex to inhibit glucose production. Cell Metab. *16*, 500–510.

Filippi, B.M., Bassiri, A., Abraham, M.A., Duca, F.A., Yue, J.T.Y., and Lam, T.K.T. (2014). Insulin signals through the dorsal vagal complex to regulate energy balance. Diabetes *63*, 892–899.

Filippi, B.M., Abraham, M.A., Silva, P.N., Rasti, M., LaPierre, M.P., Bauer, P.V., Rocheleau, J.V., and Lam, T.K.T. (2017). Dynamin-related protein 1-dependent mitochondrial fission changes in the dorsal vagal complex regulate insulin action. Cell Rep. *18*, 2301–2309.

Frizzell, R.T., Jones, E.M., Davis, S.N., Biggers, D.W., Myers, S.R., Connolly, C.C., Neal, D.W., Jaspan, J.B., and Cherrington, A.D. (1993). Counterregulation during hypoglycemia is directed by widespread brain regions. Diabetes *42*, 1253–1261.

Fu, S., Watkins, S.M., and Hotamisligil, G.S. (2012). The role of endoplasmic reticulum in hepatic lipid homeostasis and stress signaling. Cell Metab. *15*, 623–634.

Gonzàlez, J.A., Reimann, F., and Burdakov, D. (2009). Dissociation between sensing and metabolism of glucose in sugar sensing neurones. J. Physiol. *587*, 41–48.

Grayson, B.E., Seeley, R.J., and Sandoval, D.A. (2013). Wired on sugar: the role of the CNS in the regulation of glucose homeostasis. Nat. Rev. Neurosci. *14*, 24–37.

Grill, H.J., and Hayes, M.R. (2012). Hindbrain neurons as an essential hub in the neuroanatomically distributed control of energy balance. Cell Metab. *16*, 296–309.

Gujar, A.D., Ibrahim, B.A., Tamrakar, P., Cherian, A.K., and Briski, K.P. (2014). Hindbrain lactostasis regulates hypothalamic AMPK activity and metabolic neurotransmitter mRNA and protein responses to hypoglycemia. Am. J. Physiol. Regul. Integr. Comp. Physiol. *306*, R457–R469.

Hawkins, M., Gabriely, I., Wozniak, R., Reddy, K., Rossetti, L., and Shamoon, H. (2002). Glycemic control determines hepatic and peripheral glucose effectiveness in type 2 diabetic subjects. Diabetes *51*, 2179–2189.

Hackl, M.T., Furnsinn, C., Schuh, C.M., Krssak, M., Carli, F., Guerra, S., Fredenthaler, A., Baumgartner-Parzer, S., Helbich, T.H., Luger, A., et al. (2019). Brain leptin reduces liver lipids by increasing hepatic triglcyeride secretion and lowering lipogenesis. Nat. Commun. *10*, 2717.

Hayes, M.R., Skibicka, K.P., and Grill, H.J. (2008). Caudal brainstem processing is sufficient for behavioral, sympathetic, and parasympathetic responses driven by peripheral and hindbrain glucagon-like-peptide-1 receptor stimulation. Endocrinology *149*, 4059–4068.

Hayes, M.R., Bradley, L., and Grill, H.J. (2009). Endogenous hindbrain glucagon-like peptide-1 receptor activation contributes to the control of food intake by mediating gastric satiation signaling. Endocrinology *150*, 2654–2659.

Hayes, M.R., Skibicka, K.P., Leichner, T.M., Guarnieri, D.J., DiLeone, R.J., Bence, K.K., and Grill, H.J. (2010). Endogenous leptin signaling in the caudal nucleus tractus solitarius and area postrema is required for energy balance regulation. Cell Metab. *11*, 77–83.

Heni, M., Wagner, R., Kullmann, S., Veit, R., Mat Husin, H., Linder, K., Benkendorff, C., Peter, A., Stefan, N., Häring, H.-U., et al. (2014). Central insulin administration improves whole-body insulin sensitivity via hypothalamus and parasympathetic outputs in men. Diabetes *63*, 4083–4088.

Himmi, T., Perrin, J., Dallaporta, M., and Orsini, J.C. (2001). Effects of lactate on glucose-sensing neurons in the solitary tract nucleus. Physiol. Behav. *74*, 391–397.

Hirasawa, A., Tsumaya, K., Awaji, T., Katsuma, S., Adachi, T., Yamada, M., Sugimoto, Y., Miyazaki, S., and Tsujimoto, G. (2005). Free fatty acids regulate gut incretin glucagon-like peptide-1 secretion through GPR120. Nat. Med. *11*, 90–94.

Iakoubov, R., Izzo, A., Yeung, A., Whiteside, C.I., and Brubaker, P.L. (2005). Protein Kinase Cζ Is Required for Oleic Acid-Induced Secretion of Glucagon-like Peptide-1 by Intestinal Endocrine L Cells. Endocrinology *148*, 1089–1098.

Jais, A., Solas, M., Backes, H., Chaurasia, B., Kleinridders, A., Theurich, S., Mauer, J., Steculorum, S.M., Hampel, B., Goldau, J., et al. (2016). Myeloid-cell-derived VEGF maintains brain glucose uptake and Limits cognitive impairment in obesity. Cell *165*, 882–895.

Jiang, C., Xie, C., Lv, Y., Li, J., Krausz, K.W., Shi, J., Brocker, C.N., Desai, D., Amin, S.G., Bisson, W.H., et al. (2015). Intestine-selective farnesoid X receptor inhibition improves obesity-related metabolic dysfunction. Nat. Commun. *6*, 10166.

Kanoski, S.E., Zhao, S., Guarnieri, D.J., DiLeone, R.J., Yan, J., De Jonghe, B.C., Bence, K.K., Hayes, M.R., and Grill, H.J. (2012). Endogenous leptin receptor signaling in the medial nucleus tractus solitarius affects meal size and potentiates intestinal satiation signals. Am. J. Physiol. Endocrinol. Metab. *303*, E496–E503.

Kishore, P., Boucai, L., Zhang, K., Li, W., Koppaka, S., Kehlenbrink, S., Schiwek, A., Esterson, Y.B., Mehta, D., Bursheh, S., et al. (2011). Activation of K(ATP) channels suppresses glucose production in humans. J. Clin. Invest. *121*, 4916–4920.

Koch, L., Wunderlich, F.T., Seibler, J., Könner, A.C., Hampel, B., Irlenbusch, S., Brabant, G., Kahn, C.R., Schwenk, F., and Brüning, J.C. (2008). Central insulin action regulates peripheral glucose and fat metabolism in mice. J. Clin. Invest. *118*, 2132–2147.

Kuhre, R.E., Frost, C.R., Svendsen, B., and Holst, J.J. (2015). Molecular mechanisms of glucose-stimulated GLP-1 secretion from perfused rat small intestine. Diabetes *64*, 370–382.

Lam, C.K.L., Chari, M., Su, B.B., Cheung, G.W.C., Kokorovic, A., Yang, C.S., Wang, P.Y.T., Lai, T.Y.Y., and Lam, T.K.T. (2010). Activation of N-methyl-D-aspartate (NMDA) receptors in the dorsal vagal complex lowers glucose production. J. Biol. Chem. *285*, 21913–21921.

Lam, C.K.L., Chari, M., Rutter, G.A., and Lam, T.K.T. (2011). Hypothalamic nutrient sensing activates a forebrain-hindbrain neuronal circuit to regulate glucose production in vivo. Diabetes *60*, 107–113.

Lam, T.K.T., van de Werve, G., and Giacca, A. (2003). Free fatty acids increase basal hepatic glucose production and induce hepatic insulin resistance at different sites. Am. J. Physiol. Endocrinol. Metab. *284*, E281–E290.

Lam, T.K.T., Gutierrez-Juarez, R., Pocai, A., and Rossetti, L. (2005a). Regulation of blood glucose by hypothalamic pyruvate metabolism. Science *309*, 943–947.

Lam, T.K.T., Pocai, A., Gutierrez-Juarez, R., Obici, S., Bryan, J., Aguilar-Bryan, L., Schwartz, G.J., and Rossetti, L. (2005b). Hypothalamic sensing of circulating fatty acids is required for glucose homeostasis. Nat. Med. *11*, 320–327.

Lam, T.K.T., Gutierrez-Juarez, R., Pocai, A., Bhanot, S., Tso, P., Schwartz, G.J., and Rossetti, L. (2007). Brain glucose metabolism controls the hepatic secretion of triglyceride-rich lipoproteins. Nat. Med. *13*, 171–180.

LaPierre, M.P., Abraham, M.A., Yue, J.T.Y., Filippi, B.M., and Lam, T.K.T. (2015). Glucagon signalling in the dorsal vagal complex is sufficient and necessary for high-protein feeding to regulate glucose homeostasis in vivo. EMBO Rep. *16*, 1299–1307.

Laughton, J.D., Charnay, Y., Belloir, B., Pellerin, L., Magistretti, P.J., and Bouras, C. (2000). Differential messenger RNA distribution of lactate dehydrogenase LDH-1 and LDH-5

isoforms in the rat brain. Neuroscience *96*, 619–625.

Leckstrom, A., Lew, P.S., Poritsanos, N.J., and Mizuno, T.M. (2011). Central melanocortin receptor agonist reduces hepatic lipogenic gene expression in streptozotocin-induced diabetic mice. Life Sci. *88*, 664–669.

Li, A.-J., Wang, Q., Dinh, T.T., Powers, B.R., and Ritter, S. (2013). Stimulation of feeding by three different glucose-sensing mechanisms requires hindbrain catecholamine neurons. Am. J. Physiol. Regul. Integr. Comp. Physiol. *306*, R257–R264.

Li, Y., Tian, M., Yang, M., Yang, G., Chen, J., Wang, H., Liu, D., Wang, H., Deng, W., Zhu, Z., et al. (2020). Central Sfrp5 regulates hepatic glucose flux and VLDL-triglyceride secretion. Metab. Clin. Exp. *103*, 154029.

Liu, L., Karkanias, G.B., Morales, J.C., Hawkins, M., Barzilai, N., Wang, J., and Rossetti, L. (1998). Intracerebroventricular leptin regulates hepatic but not peripheral glucose fluxes. J. Biol. Chem. *273*, 31160–31167.

McDougal, D.H., Hermann, G.E., and Rogers, R.C. (2013). Astrocytes in the nucleus of the solitary tract are activated by low glucose or glucoprivation: evidence for glial involvement in glucose homeostasis. Front. Neurosci. *7*, 249.

Mizuno, Y., and Oomura, Y. (1984). Glucose responding neurons in the nucleus tractus solitarius of the rat: in vitro study. Brain Res. *307*, 109–116.

Moriya, R., Shirakura, T., Ito, J., Mashiko, S., and Seo, T. (2009). Activation of sodium-glucose cotransporter 1 ameliorates hyperglycemia by mediating incretin secretion in mice. Am. J. Physiol. Endocrinol. Metab. *297*, E1358–E1365.

Morton, G.J., and Schwartz, M.W. (2011). Leptin and the central nervous system control of glucose metabolism. Physiol. Rev. *91*, 389–411.

Morton, G.J., Matsen, M.E., Bracy, D.P., Meek, T.H., Nguyen, H.T., Stefanovski, D., Bergman, R.N., Wasserman, D.H., and Schwartz, M.W. (2013). FGF19 action in the brain induces' ' insulin-independent glucose lowering. J. Clin. Invest. *123*, 4799–4808.

Nogueiras, R., Wiedmer, P., Perez-Tilve, D., Veyrat-Durebex, C., Keogh, J.M., Sutton, G.M., Pfluger, P.T., Castaneda, T.R., Neschen, S., Hofmann, S.M., et al. (2007). The central melanocortin system directly controls peripheral lipid metabolism. J. Clin. Invest. *117*, 3475–3488.

Nogueiras, R., López, M., and Diéguez, C. (2010). Regulation of lipid metabolism by energy availability: a role for the central nervous system. Obes. Rev. *11*, 185–201.

O'Malley, D., Reimann, F., Simpson, A.K., and Gribble, F.M. (2006). Sodium-coupled glucose cotransporters contribute to hypothalamic glucose sensing. Diabetes *55*, 3381–3386.

Obici, S., Feng, Z., Tan, J., Liu, L., Karkanias, G., and Rossetti, L. (2001). Central melanocortin receptors regulate insulin action. J. Clin. Invest. *108*, 1079–1085.

Obici, S., Zhang, B.B., Karkanias, G., and Rossetti, L. (2002a). Hypothalamic insulin signaling is required for inhibition of glucose production. Nat. Med. *8*, 1376–1382.

Obici, S., Feng, Z., Morgan, K., Stein, D., Karkanias, G., and Rossetti, L. (2002b). Central administration of oleic acid inhibits glucose production and food intake. Diabetes *51*, 271–275.

Ono, H., Pocai, A., Wang, Y., Sakoda, H., Asano, T., Backer, J.M., Schwartz, G.J., and Rossetti, L. (2008). Activation of hypothalamic S6 kinase mediates diet-induced hepatic insulin resistance in rats. J. Clin. Invest. *118*, 2959–2968.

Parton, L.E., Ye, C.P., Coppari, R., Enriori, P.J., Choi, B., Zhang, C.-Y., Xu, C., Vianna, C.R., Balthasar, N., Lee, C.E., et al. (2007). Glucose sensing by POMC neurons regulates glucose homeostasis and is impaired in obesity. Nature *449*, 228–232.

Patel, B., New, L.E., Griffiths, J.C., Deuchars, J., and Filippi, B.M. (2021). Inhibition of mitochondrial fission and iNOS in the dorsal vagal complex protects from overeating and weight gain. Mol. Metab. *43*, 101123.

Patil, G.D., and Briski, K.P. (2005). Lactate is a critical "sensed" variable in caudal hindbrain monitoring of CNS metabolic stasis. Am. J. Physiol. Regul. Integr. Comp. Physiol. *289*, R1777–R1786.

Pellerin, L., and Magistretti, P.J. (1994). Glutamate uptake into astrocytes stimulates aerobic glycolysis: a mechanism coupling neuronal activity to glucose utilization. Proc. Natl. Acad. Sci. U S A *91*, 10625–10629.

Pocai, A., Lam, T.K.T., Gutierrez-Juarez, R., Obici, S., Schwartz, G.J., Bryan, J., Aguilar-Bryan, L., and Rossetti, L. (2005). Hypothalamic K(ATP) channels control hepatic glucose production. Nature *434*, 1026–1031.

Pocai, A., Lam, T.K.T., Obici, S., Gutierrez-Juarez, R., Muse, E.D., Arduini, A., and Rossetti, L. (2006). Restoration of hypothalamic lipid sensing normalizes energy and glucose homeostasis in overfed rats. J. Clin. Invest. *116*, 1081–1091.

Poppe, R., Karbach, U., Gambaryan, S., Wiesinger, H., Lutzenburg, M., Kraemer, M., Witte, O.W., and Koepsell, H. (1997). Expression of the Na+-D-glucose cotransporter SGLT1 in neurons. J. Neurochem. *69*, 84–94.

Reaven, G.M., Chen, Y.D.I., and Jeppesen, J. (1993). Insulin resistance and hyperinsulinemia in individuals with small, dense low density lipoprotein particles. J. Clin. Invest. *92*, 141–146.

Ritter, S., Dinh, T.T., and Zhang, Y. (2000). Localization of hindbrain glucoreceptive sites controlling food intake and blood glucose. Brain Res. *856*, 37–47.

Roberts, B.L., Zhu, M., Zhao, H., Dillon, C., and Appleyard, S.M. (2017). High glucose increases action potential firing of catecholamine neurons in the nucleus of the solitary tract by increasing spontaneous glutamate inputs. Am. J. Physiol. Regul. Integr. Comp. Physiol. *313*, R229–R239.

Rocca, A.S., LaGreca, J., Kalitsky, J., and Brubaker, P.L. (2001). Monounsaturated fatty acid diets improve glycemic tolerance through increased secretion of glucagon-like peptide-1. Endocrinology *142*, 1148–1155.

Sandoval, D.A., Bagnol, D., Woods, S.C., D'Alessio, D.A., and Seeley, R.J. (2008). Arcuate glucagon-like peptide 1 receptors regulate glucose homeostasis but not food intake. Diabetes *57*, 2046–2054.

Scarlett, J.M., Muta, K., Brown, J.M., and Rojas, J.M. (2019). Peripheral mechanisms mediating the sustained antidiabetic action of FGF1 in the brain. Diabetes *68*, 654–664.

Scherer, T., Lindtner, C., Zielinski, E., O'Hare, J., Filatova, N., and Buettner, C. (2012). Short term voluntary overfeeding disrupts brain insulin control of adipose tissue lipolysis. J. Biol. Chem. *287*, 33061–33069.

Scherer, T., Lindtner, C., O'Hare, J., Hackl, M., Zielinski, E., Freudenthaler, A., Baumgartner-Parzer, S., Tödter, K., Heeren, J., Kršŝák, M., et al. (2016). Insulin regulates hepatic triglyceride secretion and lipid content via signaling in the brain. Diabetes *65*, 1511–1520.

Schriever, S.C., Kabra, D.G., Pfuhlmann, K., Baumann, P., Baumgart, E.V., Nagler, J., Seebacher, F., Harrison, L., Irmler, M., Kullmann, S., et al. (2020). Type 2 diabetes risk gene Dusp8 regulates hypothalamic Jnk signaling and insulin sensitivity. J. Clin. Invest. *130*, 6093–6108.

Schwartz, M.W., Seeley, R.J., Tschöp, M.H., Woods, S.C., Morton, G.J., Myers, M.G., and D'Alessio, D. (2013). Cooperation between brain and islet in glucose homeostasis and diabetes. Nature *503*, 59–66.

Sherling, D.H., Perumareddi, P., and Hennekens, C.H. (2017). Metabolic syndrome. J. Cardiovasc. Pharmacol. Ther. *22*, 365–367.

Shi, X., Chacko, S., Li, F., Li, D., Burrin, D., Chan, L., and Guan, X. (2017). Acute activation of GLP-1-expressing neurons promotes glucose homeostasis and insulin sensitivity. Mol. Metab. *6*, 1350–1359.

Stafford, J.M., Yu, F., Printz, R., Hasty, A.H., Swift, L.L., and Niswender, K.D. (2008). Central nervous system neuropeptide Y signaling modulates VLDL triglyceride secretion. Diabetes *57*, 1482–1490.

Stark, R., Reichenbach, A., Lockie, S.H., Pracht, C., Wu, Q., Tups, A., and Andrews, Z.B. (2015). Acyl ghrelin acts in the brain to control liver function and peripheral glucose homeostasis in male mice. Endocrinology *156*, 858–868.

Su, Y., Lam, T.K.T., He, W., Pocai, A., Bryan, J., Aguilar-Bryan, L., and Gutiérrez-Juárez, R. (2012). Hypothalamic leucine metabolism regulates liver glucose production. Diabetes *61*, 85–93.

Sun, L., Xie, C., Wang, G., Wu, Y., Wu, Q., Wang, X., Liu, J., Deng, Y., Xia, J., Chen, B., et al. (2018). Gut microbiota and intestinal FXR mediate the clinical benefits of metformin. Nat. Med. *24*, 1919–1929.

Taher, J., Baker, C.L., Cuizon, C., Masoudpour, H., Zhang, R., Farr, S., Naples, M., Bourdon, C., Pausova, Z., and Adeli, K. (2014). GLP-1 receptor agonism ameliorates hepatic VLDL overproduction and de novo lipogenesis in insulin resistance. Mol. Metab. *3*, 823–833.

Taher, J., Farr, S., and Adeli, K. (2017). Central nervous system regulation of hepatic lipid and lipoprotein metabolism. Curr. Opin. Lipidol. *28*, 32–38.

Thaler, J.P., Yi, C.-X., Schur, E.A., Guyenet, S.J., Hwang, B.H., Dietrich, M.O., Zhao, X., Sarruf, D.A., Izgur, V., Maravilla, K.R., et al. (2012). Obesity is associated with hypothalamic injury in rodents and humans. J. Clin. Invest. *122*, 153–162.

Theander-Carrillo, C., Wiedmer, P., Cettour-Rose, P., Nogueiras, R., Perez-Tilve, D., Pfluger, P., Castaneda, T.R., Muzzin, P., Schürmann, A., Szanto, I., et al. (2006). Ghrelin action in the brain controls adipocyte metabolism. J. Clin. Invest. *116*, 1983–1993.

Waise, T.M.Z., Dranse, H.J., and Lam, T.K.T. (2018). The metabolic role of vagal afferent innervation. Nat. Rev. Gastroenterol. Hepatol. *15*, 625–636.

Wan, S., and Browning, K.N. (2008). D-glucose modulates synaptic transmission from the central terminals of vagal afferent fibers. Am. J. Physiol. Gastrointest. Liver Physiol. *294*, G757–G763.

Wang, J., Obici, S., Morgan, K., Barzilai, N., Feng, Z., and Rossetti, L. (2001). Overfeeding rapidly induces leptin and insulin resistance. Diabetes *50*, 2786–2791.

Wang, P.Y.T., Caspi, L., Lam, C.K.L., Chari, M., Li, X., Light, P.E., Gutierrez-Juarez, R., Ang, M., Schwartz, G.J., and Lam, T.K.T. (2008). Upper intestinal lipids trigger a gut-brain-liver axis to regulate glucose production. Nature *452*, 1012–1016.

Yang, C.S., Lam, C.K.L., Chari, M., Cheung, G.W.C., Kokorovic, A., Gao, S., Leclerc, I., Rutter, G.A., and Lam, T.K.T. (2010). Hypothalamic AMP-activated protein kinase regulates glucose production. Diabetes *59*, 2435–2443.

Yang, X.J., Kow, L.M., Funabashi, T., and Mobbs, C.V. (1999). Hypothalamic glucose sensor: similarities to and differences from pancreatic beta-cell mechanisms. Diabetes *48*, 1763–1772.

Yoon, N.A., and Diano, S. (2021). Hypothalamic glucose-sensing mechanisms. Diabetologia *64*, 985–993.

Yu, A.S., Hirayama, B.A., Timbol, G., Liu, J., Diez-Sampedro, A., Kepe, V., Satyamurthy, N., Huang, S.-C., Wright, E.M., and Barrio, J.R. (2013). Regional distribution of SGLT activity in rat brain in vivo. Am. J. Physiol. Cell Physiol. *304*, C240–C247.

Yue, J.T.Y., and Lam, T.K.T. (2012). Lipid sensing and insulin resistance in the brain. Cell Metab. *15*, 646–655.

Yue, J.T.Y., Mighiu, P.I., Naples, M., Adeli, K., and Lam, T.K.T. (2012). Glycine normalizes hepatic triglyceride-rich VLDL secretion by triggering the CNS in high-fat fed rats. Circ. Res. *110*, 1345–1354.

Yue, J.T.Y., Abraham, M.A., LaPierre, M.P., Mighiu, P.I., Light, P.E., Filippi, B.M., and Lam, T.K.T. (2015). A fatty acid-dependent hypothalamic-DVC neurocircuitry that regulates hepatic secretion of triglyceride-rich lipoproteins. Nat. Commun. *6*, 5970.

Yue, J.T.Y., Abraham, M.A., Bauer, P.V., LaPierre, M.P., Wang, P., Duca, F.A., Filippi, B.M., Chan, O., and Lam, T.K.T. (2016). Inhibition of glycine transporter-1 in the dorsal vagal complex improves metabolic homeostasis in diabetes and obesity. Nat. Commun. *7*, 13501.

Zhang, Y.-L., Hernandez-Ono, A., Ko, C., Yasunaga, K., Huang, L.-S., and Ginsberg, H.N. (2004). Regulation of hepatic apolipoprotein B-lipoprotein assembly and secretion by the availability of fatty acids. I. Differential response to the delivery of fatty acids via albumin or remnant-like emulsion particles. J. Biol. Chem. *279*, 19362–19374.

Zhang, S.-Y., Li, R.J.W., Lim, Y.-M., Batchuluun, B., Liu, H., Waise, T.M.Z., and Lam, T.K.T. (2020). FXR in the dorsal vagal complex is sufficient and necessary for upper small intestinal microbiome-mediated changes of TCDCA to alter insulin action in rats. Gut, Oct 21.

Zheng, H., Stornetta, R.L., Agassandian, K., and Rinaman, L. (2015). Glutamatergic phenotype of glucagon-like peptide 1 neurons in the caudal nucleus of the solitary tract in rats. Brain Struct. Funct. *220*, 3011–3022.

iScience, Volume *24*

Supplemental information

Nutrient infusion in the dorsal vagal complex controls hepatic lipid and glucose metabolism in rats

Rosa J.W. Li, Battsetseg Batchuluun, Song-Yang Zhang, Mona A. Abraham, Beini Wang, Yu-Mi Lim, Jessica T.Y. Yue, and Tony K.T. Lam

Supplemental Information

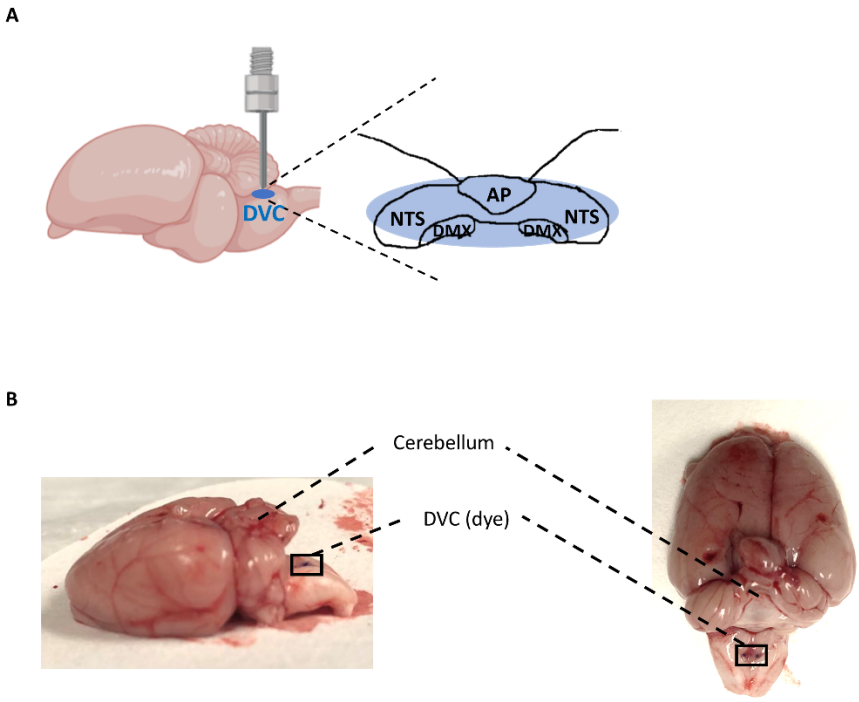

Figure S1. DVC cannula placement and dye image, Related to Figure 1 A) Anatomical location of the brain cannula inserted. DVC: dorsal vagal complex; AP: area postrema; NTS: nucleus of the solitary tract; DMX: dorsal motor nucleus of the vagus. B) Image of the brain taken after experiment with bromophenol blue dye verifying cannula placement.

TRANSPARENT METHODS

Animal preparation. Adult male Sprague Dawley rats aged ~8-10 weeks from Charles River Laboratories (Montreal, QC, Canada) were used. Rats were individually housed, subjected to a standard 12-hour light-dark (6:00 light, 18:00 dark) cycle, and had *ad libitum* access to drinking water and standard RC diet (Teklad Diet 7012, Harlan Laboratories, Madison, USA - 17% fat, 25% protein, and 58% carbohydrate; 3.1 kcal/g total metabolizable energy). For HF fed rats, animals were randomly assigned for a HFD with 10% lard oil (TestDiet 571R, Purina Mills, Richmond, USA containing 34% fat, 22% protein, and 44% carbohydrate; 3.9 kcal/g total metabolizable energy) for 3 days. Rats that did not develop hyperphagia were excluded. All animal protocols were approved by the UHN Animal Care and Use Committee in accordance with the Canadian Council on Animal Care guidelines.

Surgical procedures. Upon arrival, animals were placed under quarantine for at least two days before undergoing surgery. Rats were anaesthetized with intraperitoneal injection of ketamine (60 mg/kg; Vetalar, Bioniche, Belleville, ON) and xylazine (8 mg/kg; Rompun, Bayer, Toronto, ON) for brain cannulation surgery, where a bilateral, 26-gauge, stainless steel guide cannulae (Plastics One Inc, Roanoke, VA, USA) were stereotaxically implanted into the DVC (0.4 mm lateral to midline, 7.9 mm below cranial surface, at occipital crest). DVC region contains three distinctive nuclei, including the area postrema, the nucleus of the solitary tract, and the dorsal motor nucleus of the vagus. Of which, the brain cannula is inserted to target the nucleus of the solitary tract bilaterally (Figure S1A). At the end of experiments, we infused bromophenol blue dye through the cannula and isolated the DVC. We have validated correct placement of the brain cannula that targeted the DVC (Figure S1B). Only those data for rats that showed injection of dye within the vagal triangle (which included the area postrema, nucleus of the solitary tract, and dorsal motor nucleus that consist of the DVC) were included. The location of the DVC bilateral cannulae was also verified by infusing radioactively labelled glucose through the bilateral cannulae at 0.33 μl/hr for 210 minutes to mimic infusion rate and

duration of DVC glucose infusion in the clamp experiments. Subsequently, medio basal hypothalamus (MBH), DVC and cortex tissue were collected and counted, and radioactive counts was only identified in the targeted DVC tissue (Figure 4A). While infusion of oleic acids into the DVC for VLDL-TG experiments were 150 mins instead of 210 mins as used for the clamp studies, a shorter infusion time with lesser volume should warrant for lower probability of the infusate spreading to untargeted area. Seven days after the DVC surgery, animals are anaesthetized (ketamine, 80 mg/kg; xylazine, 10 mg/kg) for vascular surgery, where indwelling catheters were surgically implanted into the left carotid artery and right jugular vein for blood sampling and infusions. Post-surgical bodyweight and food intake were monitored. Five days following the vascular surgery on experimentation day, rats were excluded if a minimum of 90% of their pre-vascular surgery bodyweight was not attained. Rats were randomly assigned into groups before experiment.

Infusion protocol for VLDL-TG secretion experiments. Experiments were performed five days after the vascular surgery and rats were fasted for ~8-10 h. Blood sample was first collected in conscious, unrestrained rats prior to receiving DVC infusions at 0.33 μl/h (CMA 400 syringe pump, CMA Microdialysis, Inc., North Chelmsford, MA). Cyclodextrin (2.6% in saline) or oleic acid (1 mM) was infused starting t = -10 min until the end of the VLDL experiment at t = 150 min. When 1mM of oleic acid is infused into the hypothalamus of rats at the same dosage, hepatic VLDL-TG secretion is lowered (Yue et al., 2015). Triacsin C (40 μM in 5% DMSO) pre-infusion began at t = -20 min and lasted until the end of the experiment either infused alone or with oleic acid infusion beginning at t = -10 min. The concentration of triacsin C was chosen based on a previous study that documented a blockade of the ability of hypothalamic ACSL to esterify fatty acids when triacsin C was infused into the hypothalamus (Lam et al., 2005a). Pre-infusion ensures enzyme inhibition prior to infusion of substrates. FXR antagonist GMCA (500 μM) was dissolved in DMSO as stock solution (50 mM) and was diluted to 500 μM in 1% CMC as working solution. GMCA was administered as bolus at 5pm the day prior to experiment (500 μL, 1 µl/min for 2 min) as well as on the day of at t = -100 min to

achieve a 90 mins pre-exposure before vehicle or oleic acid infusion began at t = -10 min. The concentration and infusion protocol for GMCA were chosen based on a study that demonstrated when GMCA was infused at the described concentration, infusion rate, and duration into HF rats, FXR signaling in the DVC of rats was inhibited *in vivo* (Zhang et al., 2020). At t = 0 min, a blood sample was obtained after DVC pre-infusions, followed by an intravenous injection of tyloxapol (Sigma-Aldrich, St Louis, MO; 600 mg/kg, dissolved in saline) or poloxamer (Sigma-Aldrich; 600 mg/kg, dissolved in saline). Blood samples were subsequently collected every 30 min until the end of the experiment. For animals receiving intravenous infusion of saline or 20% Intralipid [20% Soybean Oil (fatty acids: linoleic (44-62%), oleic (19-30%), palmitic (7-14%), linolenic (4-11%) and stearic (1.4-5.5%)), 1.2% Egg Yolk Phospholipids, 2.25% Glycerin, and water] mixed with heparin (20 mU/ml) at 0.4 ml/hr, infusion began at the same time as DVC vehicle (5% DMSO) or triacsin C (40 μM in 5% DMSO) infusion at t = -180 min. At t = 0 min, intravenous saline or Intralipid with heparin infusion was stopped and poloxamer was intravenously injected. Blood samples were collected at t = -180, 0, and 45 min. The infusion protocol is designed based on previous studies infusing the same Intralipid mixture for 180 min and demonstrating elevation of plasma free fatty acid and TG levels as well as VLDL-TG secretion (Chapados et al., 2009; Zhang et al., 2004). Blood samples were collected into heparinized tubes and centrifuged at ~2000 × g for 30 seconds to separate the plasma, which is stored at -20 ºC until assayed. To prevent hypovolemia and anemia, packed red blood cells were resuspended in 0.2% heparinized saline and reinfused into the rat. Plasma triglycerides were measured using a commercially available kit (Roche Diagnostics, Indianapolis, IN).

Pancreatic (basal insulin)-euglycemic clamps. Rats were fasted for ~4-6 h before the clamp experiments to ensure comparable post-absorptive nutritional status. A blood sample was first collected in conscious, unrestrained rats prior to receiving DVC infusions. 0.9% saline, glucose (Sigma-Aldrich; 2 mM), or lactate (Sigma-Aldrich; 5 mM) were infused at 0.33 μl/h throughout the clamps beginning at t = 0 min to t = 210

min. Glucose concentration was chosen based on previous studies demonstrating an increase in hypothalamic glucose concentration and activation of hypothalamic glucose mechanism when glucose was infused at 2 mM into the hypothalamus (Abraham et al., 2018; Lam et al., 2005b; Yang et al., 2010). Given that one glucose molecule yields two lactate molecule and accounting for potential losses during shuttling, 5 mM was used for lactate infusion. This concentration of lactate was also used in previous studies since hypothalamic administration of lactate at 5 mM was able to lower glucose production (Yang et al., 2010). Lactate dehydrogenase blocker oxamate (Millipore Sigma; 50 mM) was first given as bolus at t = -30 min at 0.33 μl/min for 1 min, then was co-infused with glucose (2 mM) at 0.33 μl/h into the DVC throughout the clamps. Oxamate concentration and infusion protocol were based on previous studies that documented that 50 mM oxamate infusion into the hypothalamus was able to negate hypothalamic glucose sensing to lower glucose production (Abraham et al., 2018; Lam et al., 2005b). GMCA was first given as a bolus at 5pm the day prior to experiment (500 μM, 1 µl/min for 2 min) as well as on the day of at t = -90 min to achieve a 90 mins pre-exposure before saline or glucose (2 mM) infusion began at t = 0 min. Concentration of GMCA concentration and infusion protocol was explained above. Clamp methodology was performed as follows and as described (Filippi et al., 2012, 2017; Lam et al., 2011; Yue et al., 2016). At t = 0 min, a primed, continuous infusion (PHD2000 syringe pump, Harvard Apparatus, Saint Laurent, QC, Canada) of [3-^{3}H]-glucose (PerkinElmer; 40 μCi bolus + 0.4 μCi infusion) was commenced and maintained until the end of the clamp experiment at t = 210 min to measure glucose kinetics using tracer-dilution methodology. The glucose turnover was calculated using stead-state formulae, where the rate of glucose to appear in blood was calculated using [3-^{3}H]-glucose. The total rate of endogenous glucose production is equivalent to the rate of glucose utilization during the basal period (t = 60-90 min). The pancreatic (basal insulin)-euglycemic clamp was initiated at t = 90 min with primed and continuous infusion (1.5 ml/hr) of insulin (1.0 mU/kg of bodyweight/min), somatostatin (3 μg/kg/min), and a variable infusion of 25% glucose to maintain blood glucose at a similar

level to the basal period until t = 210 min. Plasma samples were collected every 10 min into heparinized tubes and centrifuged at ~2000 × g for 30 sec for the determination of [3-^{3}H]-glucose specific activity and glucose levels. Plasma glucose levels were determined by glucose oxidase method using a GM9 glucose analyzer (Analox Instruments, Stourbridge, UK). To prevent hypovolemia and anemia, packed red blood cells were resuspended in 0.2% heparinized saline and reinfused into the rat.

Pancreatic (basal insulin)-systemic Hyperglycemic clamps.

Clamp methodology was performed as follows: At t = 0 min, primed and continuous infusion of insulin (1.0 mU/kg of bodyweight/min), somatostatin (3 μg/kg/min), and a variable infusion of 25% glucose was initiated and maintained untill t = 120 min. Glucose infusion rate was adjusted to elevate plasma glucose to ~17 mM that would activate hypothalamic glucose sensing (Lam et al., 2005b). Plasma samples were collected every 10 min into heparinized tubes and centrifuged at ~2000 × g for 30 sec for the determination of glucose levels. Plasma glucose levels were determined by glucose oxidase method using a GM9 glucose analyzer. To prevent hypovolemia and anemia, packed red blood cells were resuspended in 0.2% heparinized saline and reinfused into the rat.

Measurement of radioactivity and glucose levels for brain tissues.

Tissues (MBH an DVC) were weighed, homogenized in 50 μL of buffer (2 mM Tris-HCl and 1 mM EDTA, pH=7), and centrifuged at 12500 RPM for 10 min at 4ºC. To measure radioactivity, 75 μL of supernatant was added to 4 ml of scintillation fluid and [^{3}H] was counted. To measure glucose levels, 10 μL of supernatant was pipetted into a GM9 glucose analyzer, and the glucose concentration of the homogenate was determined based on a glucose oxidase method in mg/dl. The readings were then converted to micromoles per gram of tissue.

Statistical analysis. All statistical analysis was performed using GraphPad Prism (version 8.0.1, GraphPad, La Jolla, CA, USA) based on measurements taken from distinct samples. Unpaired Student's t-test was used

in comparing two groups. One-way analysis of variance (ANOVA) with Tukey post hoc test was performed for 3+ groups and two-way ANOVA with Tukey post hoc test was performed for 3+ groups with two variables. Linear regression was used to plot plasma TG levels and calculate secretion rate. Differences were considered significant at $p < 0.05$. All numerical results are presented as mean +/- s.e.m

Supplementary References

Abraham, M.A., Rasti, M., Bauer, P.V., and Lam, T.K.T. (2018). Leptin enhances hypothalamic lactate dehydrogenase A (LDHA)-dependent glucose sensing to lower glucose production in high-fat-fed rats. J. Biol. Chem. *293*, 4159–4166.

Chapados, N.A., Seelaender, M., Levy, E., and Lavoie, J.M. (2009). Effects of exercise training on hepatic microsomal triglyceride transfer protein content in rats. Horm Metab Res *41*, 287–293.

Filippi, B.M., Yang, C.S., Tang, C., and Lam, T.K.T. (2012). Insulin activates Erk1/2 signaling in the dorsal vagal complex to inhibit glucose production. Cell Metab. *16*, 500–510.

Filippi, B.M., Abraham, M.A., Silva, P.N., Rasti, M., LaPierre, M.P., Bauer, P.V., Rocheleau, J.V., and Lam, T.K.T. (2017). Dynamin-Related Protein 1-Dependent Mitochondrial Fission Changes in the Dorsal Vagal Complex Regulate Insulin Action. Cell Rep. *18*, 2301–2309.

Lam, C.K.L., Chari, M., Rutter, G.A., and Lam, T.K.T. (2011). Hypothalamic nutrient sensing activates a forebrain-hindbrain neuronal circuit to regulate glucose production in vivo. Diabetes *60*, 107–113.

Lam, T.K.T., Pocai, A., Gutierrez-Juarez, R., Obici, S., Bryan, J., Aguilar-Bryan, L., Schwartz, G.J., and Rossetti, L. (2005a). Hypothalamic sensing of circulating fatty acids is required for glucose homeostasis. Nat. Med. *11*, 320–327.

Lam, T.K.T., Gutierrez-Juarez, R., Pocai, A., and Rossetti, L. (2005b). Regulation of blood glucose by hypothalamic pyruvate metabolism. Science *309*, 943–947.

Yang, C.S., Lam, C.K.L., Chari, M., Cheung, G.W.C., Kokorovic, A., Gao, S., Leclerc, I., Rutter, G.A., and Lam, T.K.T. (2010). Hypothalamic AMP-activated protein kinase regulates glucose production. Diabetes *59*, 2435–2443.

Yue, J.T.Y., Abraham, M.A., LaPierre, M.P., Mighiu, P.I., Light, P.E., Filippi, B.M., and Lam, T.K.T. (2015). A fatty acid-dependent hypothalamic-DVC neurocircuitry that regulates hepatic secretion of triglyceride-rich lipoproteins. Nat. Commun. *6*, 5970.

Yue, J.T.Y., Abraham, M.A., Bauer, P.V., LaPierre, M.P., Wang, P., Duca, F.A., Filippi, B.M., Chan, O., and Lam, T.K.T. (2016). Inhibition of glycine transporter-1 in the dorsal vagal complex improves metabolic homeostasis in diabetes and obesity. Nat. Commun. *7*, 13501.

Zhang, S.-Y., Li, R.J.W., Lim, Y.-M., Batchuluun, B., Liu, H., Waise, T.M.Z., and Lam, T.K.T. (2020). FXR in the dorsal vagal complex is sufficient and necessary for upper small intestinal microbiome-mediated changes of TCDCA to alter insulin action in rats. Gut.

Zhang, Y.-L., Hernandez-Ono, A., Ko, C., Yasunaga, K., Huang, L.-S., and Ginsberg, H.N. (2004). Regulation of hepatic apolipoprotein B-lipoprotein assembly and secretion by the availability of fatty acids. I. Differential response to the delivery of fatty acids via albumin or remnant-like emulsion particles. J. Biol. Chem. *279*, 19362–19374.